

# Ediacaran and Cambrian rocks on Scatarie Island and nearby Hay Island, Avalonian Mira terrane, Cape Breton Island, Nova Scotia, Canada

SANDRA M. BARR<sup>1\*</sup>, CHRIS E. WHITE<sup>2</sup>, SÖREN JENSEN<sup>3</sup>, TEODORO PALACIOS<sup>3</sup>, AND DEANNE VAN ROOYEN<sup>4</sup>

1. Department of Earth & Environmental Science, Acadia University, Wolfville, Nova Scotia B4P 2R6, Canada
2. Nova Scotia Department of Energy and Mines, Halifax, Nova Scotia B3J 2T9, Canada
2. Área de Paleontología, Facultad de Ciencias, Universidad de Extremadura, 06006 Badajoz, Spain
4. Department of Mathematics, Physics, & Geology, Cape Breton University, Sydney, Nova Scotia B1P 6L2, Canada

\*Corresponding author: <sandra.barr@acadiau.ca>

Date received: 30 July 2020 † Date accepted: 13 September 2020

## ABSTRACT

Scatarie Island and adjacent Hay Island, located 2 km east of the eastern tip of the Avalonian Mira terrane of southern Cape Breton Island, Nova Scotia, contain a succession of epiclastic and other sedimentary rocks of inferred Ediacaran to Cambrian age. The age assignment was based previously on lithological comparison with the Main-à-Dieu Group and overlying Bengal Road and MacCodrum formations of the Mira River Group. Detrital zircon grains from two sandstone samples from the Bengal Road Formation yielded typical Avalonian detrital zircon spectra with middle to late Neoproterozoic, Meso- to Paleoproterozoic (1300–2200 Ma) and Neoproterozoic ages. They indicate maximum depositional ages of  $532.4 \pm 4.2$  Ma and  $525.4 \pm 2.4$  Ma from essentially the same stratigraphic level, consistent with the interpretation that the rocks are Cambrian. The Bengal Road Formation also yielded scarce organic-walled microfossils including an acanthomorphic acritarch identified as *Polygonium* sp., also consistent with Cambrian age. The fine-grained siliciclastic succession on Hay Island, tentatively attributed to the MacCodrum Formation, yielded trace fossils, including *Teichichnus* isp. and *Gyrolithes scintillus*, that confirm Cambrian age. The Hay Island *Gyrolithes scintillus* expands the geographical distribution of this ichnospecies, previously known mainly from the Chapel Island Formation of Newfoundland, and represents a younger occurrence.

---

## RÉSUMÉ

L'île Scatarie et l'île Hay voisine, situées à deux kilomètres à l'est de la pointe du terrane avalonien Mira dans le sud de l'île du Cap-Breton en Nouvelle-Écosse, abritent une succession de roches épicastiques et d'autres roches sédimentaires remontant présumément à la période de l'Édiacarien au Cambrien. L'âge attribué était antérieurement basé sur une comparaison lithologique avec le groupe Main-à-Dieu et les formations sus-jacentes de Bengal Road et de MacCodrum du groupe de la rivière Mira. Des grains de zircon détritique provenant de deux échantillons de grès de la Formation de Bengal Road ont affiché des spectres de zircon détritique avaloniens typiques des périodes du Néoprotozoïque moyen à tardif, du Mésoprotozoïque au Paléoprotozoïque (1300 à 2200 Ma) et du Néoprotozoïque. Ils signalent des âges de sédimentation maximaux de  $532,4 \pm 4,2$  Ma et de  $525,4 \pm 2,4$  Ma d'un niveau stratigraphique essentiellement identique, ce qui correspond à l'interprétation situant les roches au Cambrien. La Formation de Bengal Road a de plus révélé la présence de microfossiles palynomorphes, notamment un acritarce acanthomorphe identifié en tant que l'espèce *Polygonium*, ce qui correspond également à l'époque du Cambrien. La succession siloclastique à grains fins sur l'île Hay, rattachée à la Formation de MacCodrum, a présenté des ichnofossiles, par exemple, l'ichnoespèce *Teichichnus* et le *Gyrolithes scintillus*, qui confirment l'âge du Cambrien. Le *Gyrolithes scintillus* de l'île Hay élargit la distribution géographique de cette ichnoespèce, antérieurement reconnue comme une espèce principalement présente dans la Formation de Chapel Island de Terre-Neuve, et il représente une occurrence plus récente.

[Traduit par la rédaction]

## INTRODUCTION

Scatarie Island is a Nova Scotia Wilderness Protected area ([https://novascotia.ca/nse/protectedareas/wa\\_scatarie.asp](https://novascotia.ca/nse/protectedareas/wa_scatarie.asp)) located in the Cabot Strait 2 km from the southeastern tip of Cape Breton Island (Fig. 1). The island has a long history as a fishing settlement, and archaeological research has provided evidence for 18th century fishing activity on the island; tales abound of life there in the Nineteenth and Twentieth centuries. The area is also known for its long history of shipwrecks, most recently the Great Lakes freighter *M.V. Miner*, which ran aground when a towing cable broke in September 2011 and which was removed from the island in 2015 (<https://novascotia.ca/news/release/?id=20150622003>).

Although designated a protected area because of its rare or unusual flora, the bedrock geology on Scatarie Island is also remarkable because it includes a rare occurrence of rocks that formed during a time interval that spans the boundary between the Ediacaran and Cambrian periods of geological time (Barr *et al.* 1992, 1996). Although much of the interior of the island consists of dense spruce and fir forest, barrens, and bogs and hence lacks outcrop, the Ediacaran–Cambrian rocks are well exposed along parts of the shoreline. The purpose of this paper is to present the first direct paleontological and U–Pb zircon evidence that rocks formed during the Ediacaran/Cambrian transition are exposed on the eastern part of Scatarie Island and adjacent Hay Island (Fig. 2).

## REGIONAL BACKGROUND

Southeastern Cape Breton Island, geologically comprising the Mira terrane (Barr and Raeside 1989), is part of Avalonia in the northern Appalachian orogen (Fig. 1, inset). Like other parts of Avalonia, the Mira terrane is characterized by Neoproterozoic volcanic, sedimentary, and plutonic rocks, overlain by lower Paleozoic sedimentary rocks (Fig. 1). Weeks (1954) included all the Precambrian volcanic and sedimentary rocks in a single unit called the Fourchu Group; but based on mapping, petrological studies, and U–Pb zircon dating, Barr *et al.* (1992, 1996) subdivided the rocks into groups of three different ages, ca. 680 Ma, ca. 620 Ma, and ca. 575 Ma (Fig. 1). The name Fourchu Group was retained only for the ca. 575 Ma volcanic and minor sedimentary rocks in the coastal part of the terrane south of Louisbourg. The new name Main-à-Dieu Group was assigned to rocks west, north, and east of Louisbourg that were considered equivalent in age to and/or younger than the Fourchu Group on the basis of field relations, petrological characteristics, and a poorly constrained U–Pb zircon age of <560 Ma from a rhyolite sample (Bevier *et al.* 1993). Other group names were assigned to volcanic, volcanoclastic, and sedimentary rocks farther south and west in the terrane, based mainly on U–Pb zircon ages from volcanic rocks and associated plutons (Fig. 1). Subsequently, formation names were introduced for lithological units within each of these groups by Barr and White (2017a, b).

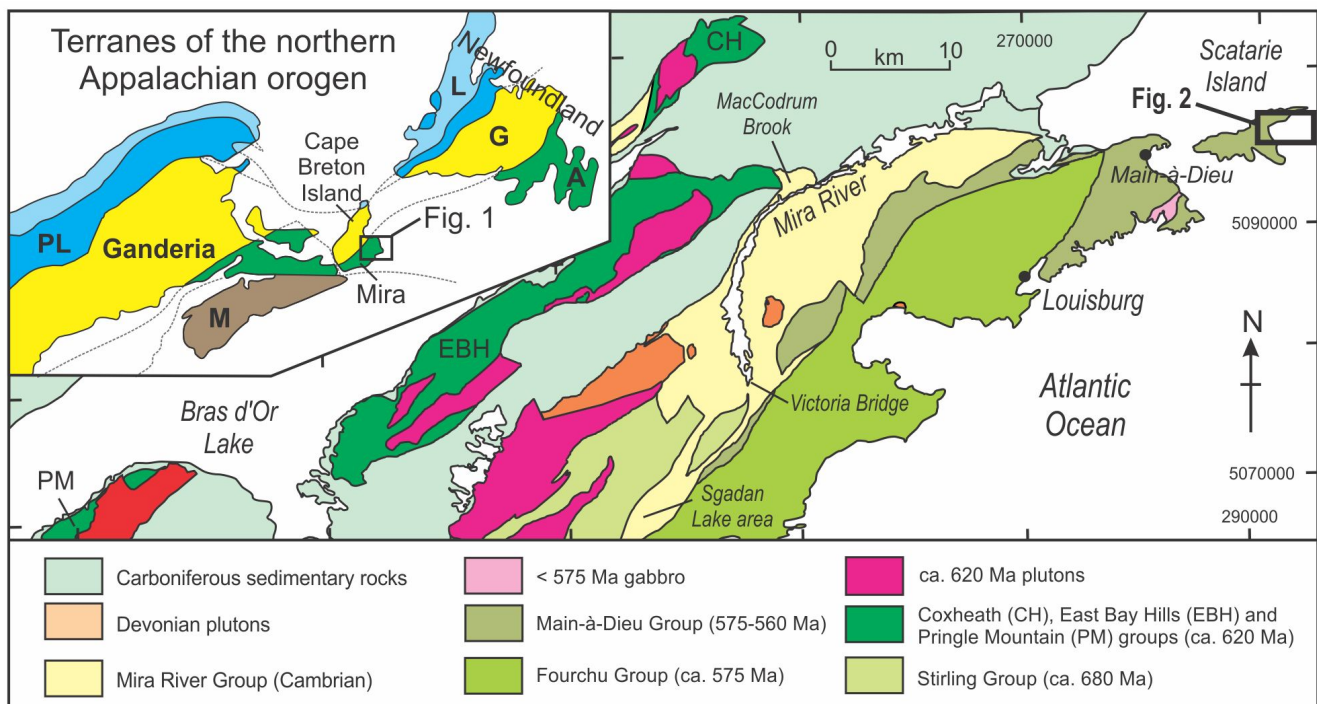


**Figure 1.** Simplified geological map of the northern part of the Mira terrane, southeastern Cape Breton Island, modified from Barr *et al.* (1996), showing the distribution of Neoproterozoic, Cambrian, and Carboniferous rocks and the location of Scatarie Island. Inset map shows the location of the Mira terrane and map area in the context of northern Appalachian terranes, modified from Hibbard *et al.* (2006). A = Avalonia, G = Ganderia, L = Laurentian margin, M = Meguma, PL = peri-Laurentian arcs.

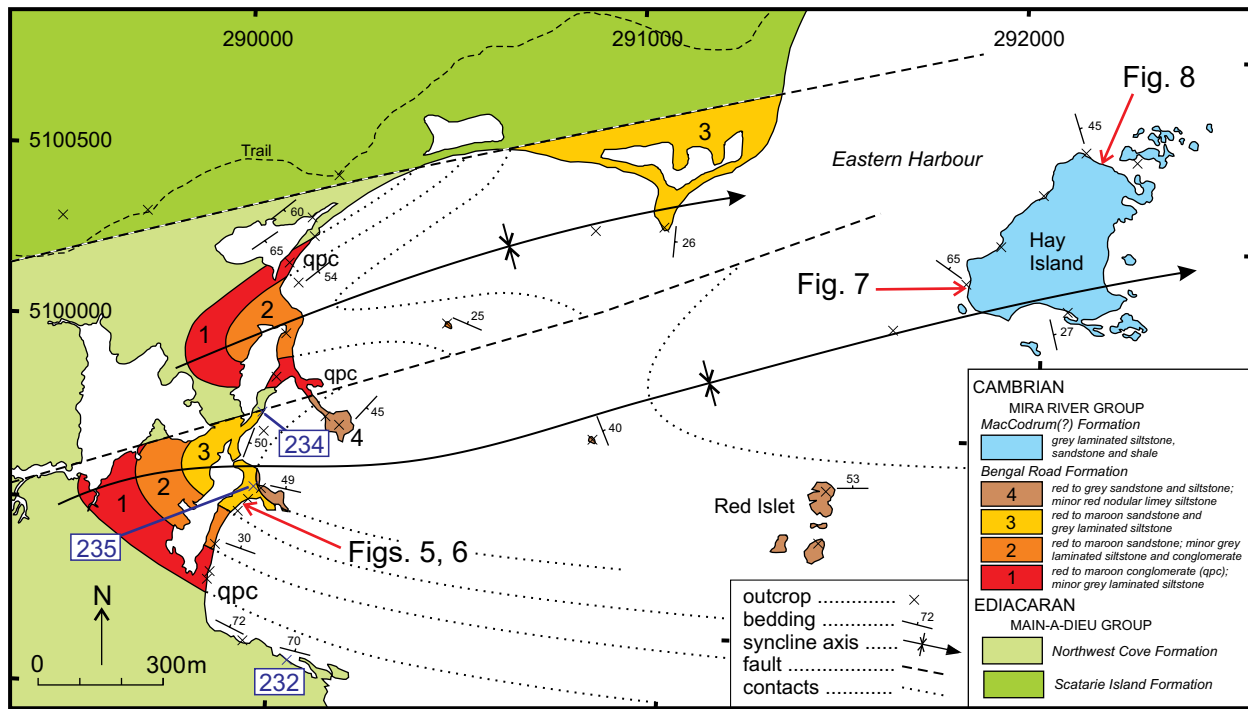


**Figure 2.** Geological map of the southeastern part of Scatarie Island and nearby Hay Island modified from Barr and White (2017a, b, c). Locations of dated samples SMB17-234 and 235 are shown in member 3 of the Bengal Road Formation, as well as sample SMB17-232 from the underlying Northwest Cove Formation which lacked zircon. Also shown are locations of photographed specimens in Figs. 6–8. Location for sample SMB17-232 = Grid Zone 21T (WGS84) 289998 5099504

The Cambrian sedimentary rocks that locally overlie the Neoproterozoic volcanic, sedimentary, and plutonic rocks form a broadly synclinal structure in the Mira River area, and Barr and White (2017a, b) referred to them collectively as the Mira River Group. Hutchinson (1952) and Weeks (1954) divided Cambrian sedimentary rocks into six formations: Morrison River, MacCodrum, Canoe Brook, Trout Brook, MacLean, and McNeil. Barr *et al.* (1992, 1996) retained these formation names except for Morrison River, which they replaced by the Bengal Road and Sgadan Lake formations because they considered the latter to be mappable units distinct from the red beds in the underlying Main-à-Dieu Group, all of which had been included previously in the Morrison River Formation (Weeks 1954).

As defined by Barr *et al.* (1992, 1996), the Bengal Road Formation is a dominantly red clastic sedimentary unit that overlies volcanic and sedimentary rocks of the Main-à-Dieu Group. Contacts are mainly faults or are unexposed, but an originally disconformable relationship is most likely. The Bengal Road Formation differs from sedimentary units of the underlying Main-à-Dieu Group in that the former contains abundant detrital muscovite and lacks volcanic and volcanoclastic rocks. It also contains a distinctive quartzite-quartz-pebble conglomerate unit at or near its base, and is interlayered with, and overlain by, red sandstone and siltstone, commonly with well-developed cross-bedding and graded bedding. Landing (1991) correlated this red bed unit of the Mira terrane with the late Ediacaran Rencontre For-

mation of Newfoundland; but Barr *et al.* (1992, 2003, 2012) and Reynolds *et al.* (2009) considered it to be Cambrian based mainly on the presence of detrital muscovite and on other lithological contrasts with underlying non-micaceous red beds. Maximum depositional ages of ca. 544 and 537 Ma were reported by Willner *et al.* (2013) based on U–Pb dating of detrital zircon from the Mira River area.

The overlying Sgadan Lake Formation is a distinctive white, rarely maroon, cross-bedded quartz arenite which is locally conglomeratic with abundant quartz pebbles. The Sgadan Lake Formation in its type area near Sgadan Lake was correlated with the Random Formation of Newfoundland by Landing (1991). Landing (1991) also recognized a separate unit of shale between the red bed and quartz arenite units that he correlated with the Chapel Island Formation, which in Newfoundland occurs between the Rencontre and Random formations. Barr *et al.* (1996) also noted the presence of shale and siltstone but did not consider those rocks to constitute a separate mappable unit and so included them in their Bengal Road Formation. Barr *et al.* (2012) reported a single concordant detrital zircon age of ca. 529 Ma from the Sgadan Lake Formation in its type area, although a single analysis cannot be considered to provide a reliable maximum depositional age.

Barr *et al.* (1992, 1996) also assigned white quartz arenite and conglomerate in MacCodrum Brook to their Sgadan Lake Formation, although Landing (1991) had placed those rocks in the Rencontre Formation. The Sgadan Lake Formation

in MacCodrum Brook is overlain by the type section of the MacCodrum Formation of Hutchinson (1952). It consists of grey and green siltstone and shale, with minor sandstone intervals. Carbonate nodules are present close to the base of the formation and also higher in the section. This section is the only good exposure of this unit, because many outcrops farther south in the Mira River area originally attributed to the MacCodrum Formation by Hutchinson (1952) were later shown to belong to younger units (Landing 1991; Barr *et al.* 1996). By comparison with Newfoundland, Landing (1991) equated the type section of the MacCodrum Formation with the Bonavista Group (Cambrian Stage 2–3) and suggested that an unconformity is present between it and the underlying quartz arenite. However, Barr *et al.* (1996) observed interlayered quartz arenite and shale in some locations and hence, like Hutchinson (1952), considered that the units are conformable. Later Landing (2004) revised his earlier correlation of the type section of the MacCodrum Formation with Newfoundland units because of the higher sandstone content than found in the Bonavista Group, and instead attributed it to the Chapel Island Formation. The details of rocks in the MacCodrum Brook section are further complicated by the fact that Willner *et al.* (2013) reported a maximum depositional age of  $517 \pm 3$  Ma for the Sgadan Lake quartz arenite there, based on results from an eight-grain detrital zircon population. Results of work in progress to evaluate the implications of this young age and the details in the still-enigmatic MacCodrum Brook section will be reported in a subsequent paper.

The MacCodrum Formation is the oldest unit on Cape Breton Island that has yielded trace fossils (Landing 2004) and acritarchs (Palacios *et al.* 2015). Acritarchs from the type section on MacCodrum Brook include *Granomarginata* and *Asteridium* (Palacios *et al.* 2015). Acritarchs and trace fossils from the type section are consistent with attribution to the Fortunian or Cambrian Stage 2. The overlying Canoe Brook Formation consists of red-brown, carbonate-rich mudstone and siltstone, maroon siltstone containing grey-green reduction spots, and minor pink to red limestone. According to Landing (1991), the Canoe Brook Formation, as well as the upper part of the underlying MacCodrum Formation (as originally mapped by Hutchinson 1952), are equivalent to the Bonavista Group and Brigus Formation in Newfoundland based on lithological characteristics and skeletal fossils. The contact between the MacCodrum and Canoe Brook formations is nowhere exposed. Landing (1991) recovered skeletal fossils from the Canoe Brook Formation along the Louisbourg Highway, which he attributed to the *Camenella baltica* Zone of Cambrian Stage 3 (Geyer 2019). From the upper part of the formation, Landing (1991) reported the trace fossil *Teichichnus* and trilobite hash. Trilobites were also discovered by Hutchinson (1952), who reported the Cambrian Stage 3 *Callavia* Zone-trilobite *Strenuella strenua* from the Victoria Bridge area (Fig. 1) in rocks originally attributed to the MacCodrum Formation but now part of the Canoe Brook Formation (Barr *et al.* 1996).

The Trout Brook Formation (Hutchinson 1952), dom-

inantly dark-grey to rust-brown, well cleaved shale and siltstone, overlies the Canoe Brook Formation. Toward the stratigraphic top of the Trout Brook Formation, the shale becomes locally maroon, with thin, graded beds of fine-grained sandstone. The Trout Brook Formation contains Miaolingian trilobites (Hutchinson 1952) and acritarchs (Palacios *et al.* 2009). The MacLean Brook Formation (Hutchinson 1952) overlies the Trout Brook Formation, and consists of interbedded grey quartz sandstone, siltstone, and shale with minor light-grey quartz sandstone and maroon shale. It contains Miaolingian trilobites (Hutchinson 1952) and Miaolingian and Furongian acritarchs (Palacios *et al.* 2009). The MacLean Brook Formation appears to be conformable with the underlying shales of the Trout Brook Formation and is overlain by grey shale, siltstone, and limestone of the Furongian McNeil Formation (Hutchinson 1952).

## GEOLOGY OF SCATARIE ISLAND AND HAY ISLAND

The geology of Scatarie Island was first described by Fletcher (1879), who provided a vivid description of the island and recognized various types of “felsites” from coastal sections. He also reported a conglomerate visible at low tide on eastern Scatarie Island that he thought to be of probable Carboniferous age, subsequently assigned to the Cambrian Bengal Road Formation (Barr *et al.* 1996, 2003, this paper). Weeks (1954) included all of Scatarie Island in his Fourchu Group, based on mapping by Hayes *et al.* (1938). However, Barr and White (1989) and Barr *et al.* (1996) re-assigned most of the Scatarie Island rocks to the Main-à-Dieu Group and also recognized for the first time the presence of probable Cambrian rocks overlying the Main-à-Dieu Group on the eastern part of the island (Fig. 2).

Barr *et al.* (1996) divided the Main-à-Dieu Group on Scatarie Island into map units based on rock type, and those units were assigned formation names by Barr and White (2017a, b, c). The inferred oldest unit on the island, the Scatarie Island Formation, forms the northeastern part of the island, in faulted contact to the south with the Northwest Cove Formation and Cambrian rocks of the Bengal Cove Formation (Fig. 2). The Northwest Cove Formation is the uppermost formation in a conformable stratigraphic succession that youngs consistently to the east across Scatarie Island (Barr *et al.* 1996; Barr and White 2017c). The formation consists mainly of amygdaloidal basaltic flows interlayered with red volcanogenic conglomerate, epiclastic sandstone, and tuff.

The overlying mainly red to maroon sedimentary rocks were assigned to the Cambrian Bengal Road Formation based on lithology (Barr *et al.* 1992, 1996). The distribution of rock types, structural orientations, and well-preserved younging directions indicate that the Bengal Road Formation occurs in a faulted synclinal structure (Fig. 2). At the time of a visit in August 1991, a gap of about 10 m separated the uppermost amygdaloidal basalt flow of the Northwest

Cove Formation from an outcrop of quartzite- and quartz-pebble conglomerate, characteristic of the base of the Bengal Road Formation elsewhere in the Mira terrane (Barr *et al.* 1992). The conglomerate is repeated in three outcrops in the well-exposed section, although during our most recent visit in 2017, the southernmost outcrops observed in 1991 were not exposed. The rocks are divided into four members. The quartzite- and quartz-pebble conglomerate (member 1) grades into red to maroon sandstone with minor interbedded grey laminated siltstone and conglomerate of member 2, and then into a unit of red to maroon sandstone and grey laminated siltstone which lacks conglomerate (member 3), overlain by red to grey sandstone and siltstone with minor red nodular limey siltstone (member 4). Younging direction is clear throughout this section, and the first three members are repeated north of an east-northeast-trending fault (Fig. 2). All four members contain abundant detrital muscovite, absent from the underlying Northwest Cove Formation and other formations of the Main-à-Dieu Group.

Some control from mainly submerged rocky shoals enables the synclinal structure to be traced offshore toward Hay Island, but red beds do not occur on the island. There, the rocks are grey laminated siltstone, sandstone, and shale that appear lithologically similar to the MacCodrum Formation in the Mira River area (Barr *et al.* 1992, 1996). However, based on some lithological similarities to the Trout Brook Formation, in their more recent compilation maps Barr and White (2017c) assigned the Hay Island rocks to the Trout Brook Formation. In either case, no evidence for the white quartz arenite of the Sgadan Lake Formation, or for other intervening formations, was observed, and if present, it is hidden under water.

## U-PB GEOCHRONOLOGY

### Sample descriptions and methods

Three samples (SMB17-232, 234, and 235) were collected for U-Pb dating of detrital zircon but only the latter two contained zircon grains. Sample SMB17-232 is red pebble conglomerate from the upper part of the Northwest Cove Formation (Fig. 2). The conglomerate overlies and underlies amygdaloidal basalt flows. It contains abundant plagioclase and epidote clasts and varied lithic fragments (including volcanic glass, basalt, dacite, and rhyolite) but minor quartz and no detrital muscovite or zircon.

In contrast, samples SMB17-234 and 235, both from the red to maroon sandstone and grey laminated siltstone of member 3, contain abundant detrital muscovite, as well as zircon. SMB17-234 is red arkosic sandstone with abundant angular quartz and less abundant plagioclase clasts. Lithic clasts include both volcanic and clastic sedimentary material. Sample SMB17-235 is greywacke, finer grained than sample 234 and with more abundant muscovite. Many of the muscovite fragments had been deformed and crenulated prior to deposition. They occur with quartz and feldspar

clasts in a muddy matrix that forms about 25% of the rock.

The samples were sent to Overburden Drilling Management (Ottawa, Ontario) for electro-pulse disaggregation and zircon separation. Zircon grains in samples SMB17-234 and 235 were then handpicked, mounted on an epoxy-covered thin section, polished to expose the centres of the zircon grains, and imaged using cold cathodoluminescence to identify internal zoning and inclusions. These images were used to select ablation points (30 µm diameter), avoiding any visible inclusions, cracks, or other imperfections. Grains were analyzed by laser ablation inductively coupled plasma mass spectrometry (LA-ICP-MS) at the Department of Earth Sciences, University of New Brunswick (Appendix A: Table A1 and A2 — two runs for each sample are reported and all data from both runs are analyzed and discussed together). U and Pb isotopic compositions were measured using a Resonetics S-155-LR 193 nm Excimer laser ablation system connected to an Agilent 7700× quadrupole inductively coupled plasma-mass spectrometer, following the procedure outlined by McFarlane and Luo (2012) and Archibald *et al.* (2013). Data reduction was done in-house using Iolite software (Paton *et al.* 2011) to process the laser output into data files, and further reduced for U-Pb geochronology using VizualAge (Petrus and Kamber 2012).

Corrections are applied as follows: for grains with <100 counts/s  $^{204}\text{Pb}$ , data are uncorrected; for grains where the percentage error on the  $^{204}\text{Pb}$  counts per second was <20%, we used a  $^{204}\text{Pb}$ -based correction (Andersen 2002), and for grains where the percentage of radiogenic Pb ( $\text{Pb}^*$  in file) is less than 98.5% we used a  $^{208}\text{Pb}$ -based correction (Petrus and Kamber 2012). Data were sorted by % concordance ( $^{206}\text{Pb}/^{238}\text{U}$  versus  $^{207}\text{Pb}/^{235}\text{U}$  for grains <1000 Ma and  $^{206}\text{Pb}/^{238}\text{U}$  versus  $^{207}\text{Pb}/^{206}\text{Pb}$  for grains >1000 Ma), and by the % of radiogenic Pb in the grains as calculated using VizualAge (Appendix A: Tables A1 and A2). Concordia and weighted mean ages as well as probability distribution histograms were calculated using Isoplot version 4.15 (Ludwig 2012).

Probability distribution histograms are based on  $^{206}\text{Pb}/^{238}\text{U}$  dates for grains <1000 Ma and  $^{207}\text{Pb}/^{206}\text{Pb}$  dates for >1000 Ma and show all grains that are between 90 and 102% concordant. To determine the youngest age represented in each sample we used only clusters of more than 3 grains with ages that overlap within error and are 98–101% concordant. Using only near-concordant grains that overlap within error is a conservative approach, which serves to reduce the possibility of misrepresenting the maximum depositional age as too young by using single grains that may have experienced Pb loss (Dickinson and Gehrels 2010). Data for reference materials FC-1 and Plesovice are presented in Appendix A, Table A2, with standards for Run 1 and Run 2 shown separately.

## Results

Sample SMB17-234 contains zircon grains with a wide range of sizes between 50–300 µm, and grains of all sizes



were analyzed. Some of the larger grains are subhedral and rectangular and some are rounded and anhedral; the smaller grains are mostly subhedral to anhedral and rounded. All analyzed grains had very weak fluorescence in CL but some of the larger grains showed faint oscillatory zoning. Of 132 grains analyzed, 80 are between 90 and 102% concordant (Appendix A: Table A1). The major peak in the cumulative probability distribution is around 520–530 Ma, with minor peaks at 1.5 Ga, 1.8 Ga and 2.0 Ga and a few grains at 3.0 Ga (Figs. 3a, b). The gaps in ages at around 1000 Ma and around 2500 Ma are typical of detrital zircon signatures in Avalonia, as is the scatter of ages between about 1300 and 2100 Ma (e.g., Barr *et al.* 2012). Among the Neoproterozoic to Cambrian grains, it is possible to calculate a concordia age for 12 grains in the youngest peak at  $526.3 \pm 2.2$  Ma, but the mean square of weighted deviation (MSWD) is very high at 7.0 and has a correspondingly low probability of concordance at 0.008 (Fig. 3c). The weighted mean age for the same 12

grains is  $525.4 \pm 2.4$  Ma with a much lower MSWD of 1.11 (Fig. 3d). In this case the weighted mean age at ~525 Ma is likely the most robust estimate of the maximum depositional age for this sample.

Zircon grains in sample SMB17-235 range in size from 50–200  $\mu\text{m}$  and grains of all sizes were analyzed. Some of the larger grains are subhedral and acicular to rectangular whereas the smaller grains are mostly subhedral to anhedral and rounded. All of the grains had weak fluorescence in CL but some of the larger grains showed faint oscillatory zoning. Of 128 grains analyzed, 86 are between 90 and 102% concordant (Appendix A: Table A1). The major peak in the cumulative probability distribution is around 530 Ma, with minor peaks at 1.5 Ga, 1.8 Ga and 2.0 Ga and a few grains around 2.7 Ga and 3.4 Ga (Figs. 4a, b). Like sample SMB17-234, this sample also displays the gaps at ca. 1000 and 2500 Ma and a spread of ages between about 1300 and 2200 Ma, typical of Avalonia. For Neoproterozoic to Cambrian grains,

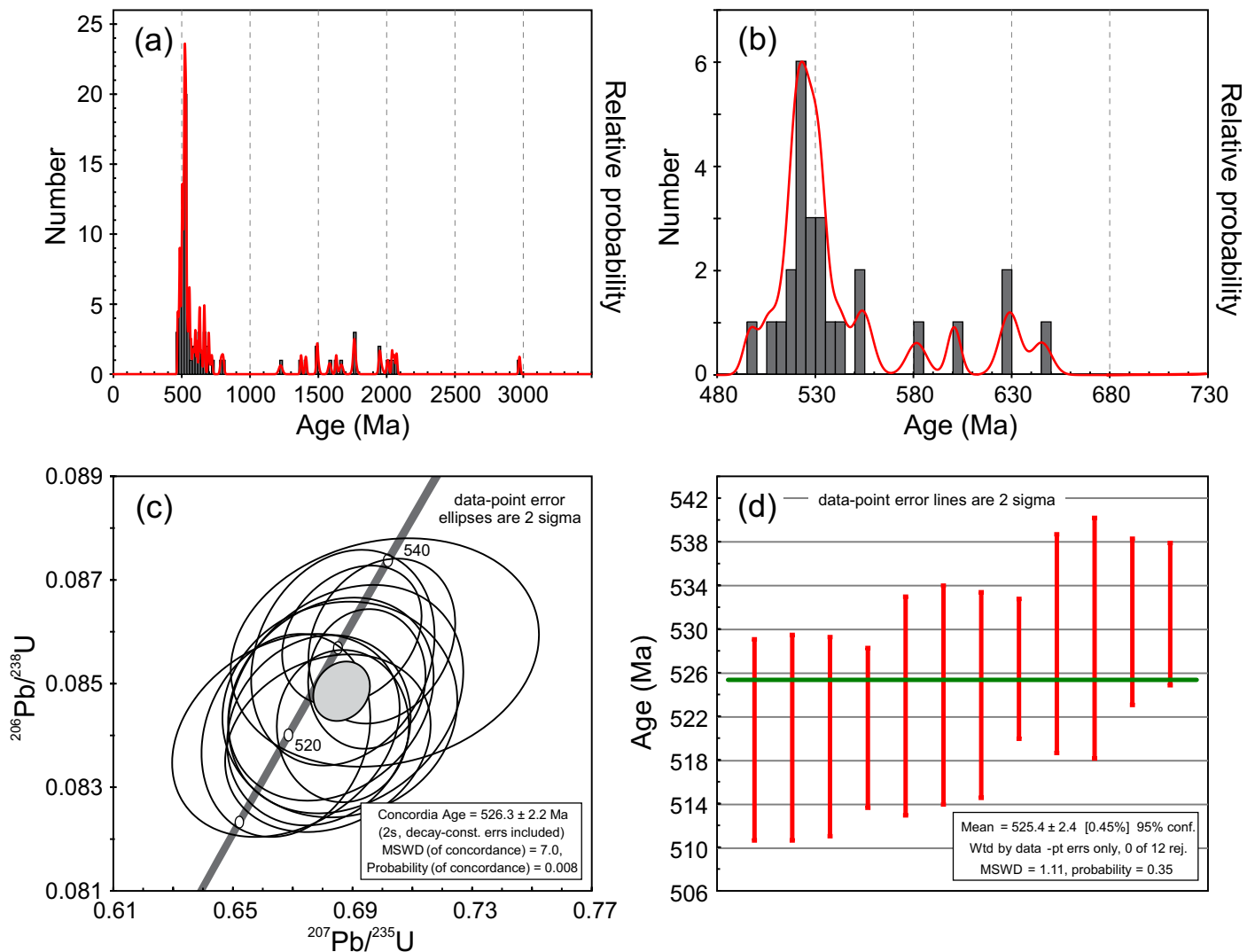


**Figure 3.** U–Pb zircon diagrams for sample SMB17-234 (data from Table A1). (a) Probability plot for all data between 90 and 102% concordant. (b) Expanded view of probability plot in (a) for ages less than 750 Ma. (c) Concordia diagram for youngest statistically valid age population. (d) Weighted mean diagram for the same 12 grains shown in (c).

three separate peaks occur on the cumulative probability distribution (Fig. 4b), but the calculated concordia age for the youngest group of 5 grains is  $534.4 \pm 3.9$  Ma with a high MSWD of 4.5 and a low probability of concordance at 0.034. The weighted mean age of the same 5 grains is  $532.4 \pm 4.2$  Ma with a much lower MSWD of 0.15 (Fig. 4d). In this case the weighted mean age is likely the most robust estimate of the maximum depositional age for this sample. The grains with ages scattered between 550 Ma and 780 Ma could all have sources within Avalonia (e.g., van Staal *et al.* 2020).

## TRACE FOSSILS AND ORGANIC-WALLED MICROFOSSILS

### Material and methods

Coastal sections on eastern Scatarie Island and on Hay

Island were examined for their fossil contents and documented by digital photography. More than 100 m of continuous outcrop of the Bengal Road Formation is accessible at low tide. As exposed in July 2017, the section commenced with about 30 m of laminated and thin-bedded, yellow- and brown-weathering grey siltstone and minor sandstone of member 2. Small-scale truncations and bedding rupture is commonly seen (Figs. 5a–c). The proportion of sandstone increases up-section into member 3 and include beds with large cubes of pyrite (Fig. 5d). Three samples of dark-grey silt-stone were collected for organic-walled microfossils from this section. Member 3 is overlain by red sandstone/siltstone of member 4 (Fig. 5e) which contains minor red nodular limey siltstone (Fig. 5f).

Outcrops tentatively attributed to the MacCodrum Formation were examined at three coastal sections on Hay Island, with a total of five samples collected for organic-walled microfossils (Fig. 2). Samples collected for organic-walled

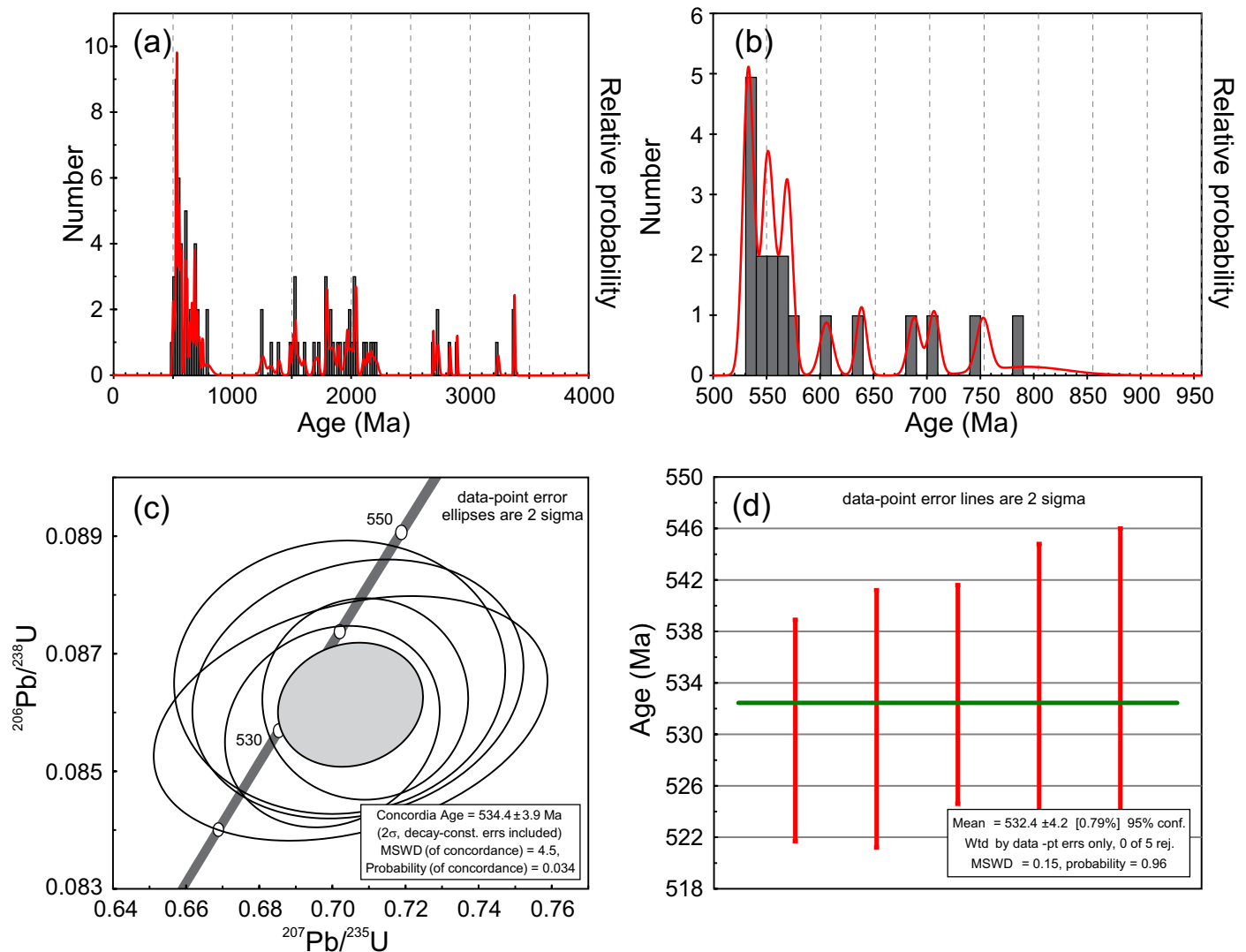


**Figure 4.** U–Pb zircon diagrams for sample SMB17-235 (data from Table A1). (a) Probability plot for all data between 90 and 102% concordant. (b) Expanded view of probability plot in (a) for ages less than 950 Ma. (c) Concordia diagram for youngest statistically valid age population. (d) Weighted mean diagram for the same 5 grains shown in (c).

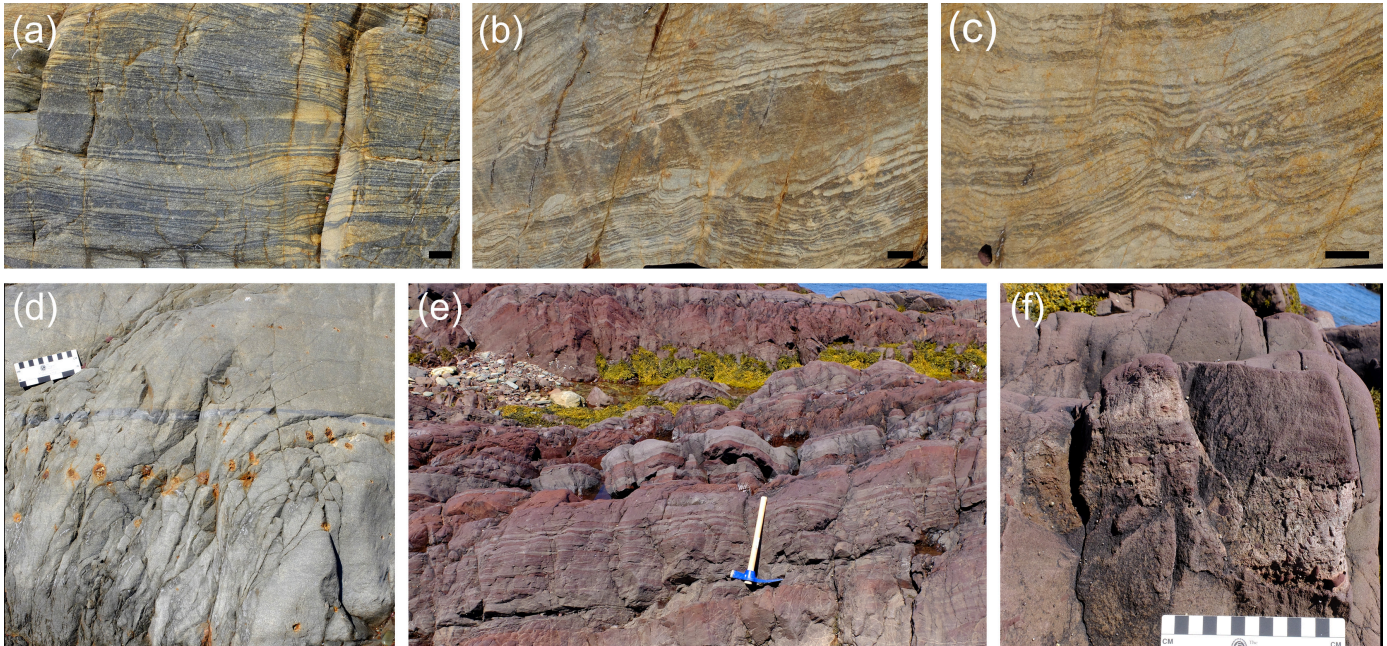


**Figure 5.** Field images of coastal exposures of the Bengal Road Formation on eastern Scatarie Island. Scale bars represent 10 mm. (a–c) Characteristic lamination and bedding in lower part of measured section of Bengal Road Formation (members 2 and 3). Samples SC17-5 and -6 were collected from fine-grained intervals in this type of rock. Deformed bedding give rise to trace fossil-like structures, particularly well seen in (c). (d) Fine-grained sandstone with large pyrite crystals. (e) Red sandstone and siltstone (member 4). (f) Red nodular limey siltstone (member 4).

microfossils were prepared and examined at Área de Paleontología, University of Extremadura, Badajoz, following palynological procedures outlined in Vidal (1988). See Appendix B for details on locations and samples. Palynological slides containing figured and representative material are stored with the collections in Nova Scotia Museum of Natural History, Halifax (museum numbers added in the explanation of the figures).

#### Results: organic-walled microfossils

All samples from Hay Island had no or only small amounts of dispersed organic material and no identifiable organic-walled microfossils (see Appendix B). Two samples from the Bengal Road Formation yielded poorly preserved organic-walled microfossils (Fig. 6). This material includes probable cyanobacterial filamentous sheaths (Fig. 6a) and organic fragments of uncertain origin. A single poorly preserved acanthomorphic acritarch (Fig. 6b) is identified as *Polygonium* sp. This acritarch does not provide biostratigraphic information beyond that of a post-Ediacaran age. Sarjeant and Stancliffe (1996) restricted *Polygonium* to the Cambrian to Devonian interval, but younger occurrences have been reported. These samples provide the first records of organic-walled microfossils from the Bengal Road Formation.

#### Results—trace fossils

No definitive trace fossils were observed in the Bengal Road Formation. Bedding-plane exposures are not well developed, which severely limits the possibility of observing any delicate bedding-plane parallel trace fossils. Angular or rod-shaped bodies seen in vertical and oblique section (Figs. 5b–c) have similarity to trace fossils but their interpretation

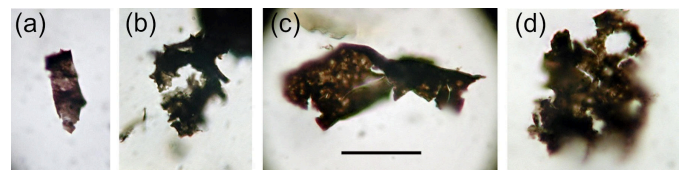


**Figure 6.** Organic-walled microfossils from Bengal Road Formation, Scatarie Island. Scale bar in c is equivalent to 20  $\mu\text{m}$  for a–d. Sample number, the Nova Scotia Museum of Natural History collection number, and England Finder coordinates (for position of microfossils on the palynological slide; <https://www.graticulesoptics.com/products/stage-micrometers-calibration-scales-grids/coordinate-graticules/s7-england-finder>) are provided. (a) Possible cyanobacterial filament, SC17-5, NSM020GF14.1, V-51-2. (b) *Polygonium* sp., SC17-6, NSM020GF14.2, J-43-1 (c) Organic-walled fragment, SC17-6, NSM020GF14.2, M-41-1. (d) Degraded organic-walled fragment, SC17-6, NSM020GF14.2, B-42-4.



is complicated by frequent small-scale (syndepositional?) disturbance, fracturing and rotation of laminae and beds. It is probable that structures such as those shown in Fig. 5c represent rotated pieces of primary sedimentary structures.

Trace fossils were observed on several coastal sections on Hay Island (Fig. 2). On the southern part of the island, outcrops of mainly grey-green and dark-grey siltstone contain examples of starved ripples of fine sandstone (Fig. 7b) and teichichnid trace fossils with clear evidence for spreite (Fig. 7a). The spreiten show at least 5 lamellae, with downward-oriented convexity, which indicates a retrusive development of the spreite, although no causative burrow was clearly identified. These trace fossils are assigned to *Teichichnus* isp.

Trace fossils were observed on weathered outcrop of cleaved grey-green siltstone on the northern tip of the island, with the most notable being small, vertically oriented, spiral trace fossils (Figs. 8a–c). These spirals are developed within silty material and filled with fine sand related to thin sandstone event beds. The best exposed specimen (Fig. 8a) has two whorls (whorl height approximately 6 mm), a burrow diameter of 0.7 mm and a spiral radius of 1.6 mm. Another less well-exposed specimen with comparable dimensions shows three whorls of the spiral (Fig. 8b). Both in dimensions and spiral geometry this material is like *Gyrolithes scintillus* from the Chapel Island Formation, Burin Peninsula, Newfoundland, as described by Laing *et al.* (2018). Other trace fossils from the Hay Island outcrop consist of short plug-shaped cones (Fig. 8d). Similar trace fossils from the Chapel Island Formation in Newfoundland

have been identified as *Conichnus*, but both the material described here and that from Newfoundland could alternatively be the fill of the funnel-shaped top of an otherwise not preserved, short, vertical trace fossil. Additional nondescript trace fossils are also present (Fig. 8e). Trace fossils in this outcrop exhibit “floating” and “adhering” preservation, similar to that commonly seen in the Chapel Island Formation of Newfoundland (Droser *et al.* 2002), in which sand-filled burrows are floating in a finer-grained matrix (Fig. 8e) or secondarily adhered to a later sand bed. A loose sample along the same stretch of outcrop show *Teichichnus* isp. and more strongly developed sediment mixing (Fig. 8f). The slab is sedimentologically similar and is interpreted as a less weathered sample from the same interval of the succession.

## DISCUSSION

Both the detrital zircon ages and fossils described here confirm a Cambrian age for the siliciclastic successions on eastern Scatarie Island and on Hay Island, a conclusion previously based on lithological correlation with the Bengal Road and MacCodrum formations, respectively, on Cape Breton Island (Barr *et al.* 1996). The maximum depositional ages of 532 and 526 Ma and the presence of the acritarch *Polygonium* sp. from the Bengal Road Formation on eastern Scatarie Island demonstrate that the upper part of this formation is definitely younger than the late Ediacaran Rencontre Formation in Newfoundland, with which the Bengal Road Formation was compared by Landing (1991, 1996). The new data reported here, combined with detrital zircon age constraints from Cape Breton Island (Barr *et al.* 2012; Willner *et al.* 2013), indicate that the Bengal Road Formation spans much of the Fortunian and Cambrian Stage 2. The age of the base of the formation is not known, nor is the duration of the inferred break in sedimentation between the Main-à-Dieu and Mira River groups. The stratigraphic position of the Bengal Road Formation could in part be equivalent to that of the Ratcliffe Brook Formation in New Brunswick, as previously suggested by Barr *et al.* (2012); if so, the base of the formation is intra-Fortunian.

The geological mapping information (Barr *et al.* 1992, 1996; this paper) indicates that the eastern coast of Scatarie Island and Hay Island are both part of the same east-plunging synclinorium (Fig. 2). Based on lithological characteristics Barr *et al.* (1996) attributed the Hay Island succession to the MacCodrum Formation, in which case the sandstone facies of the Sgadan Lake Formation either is not exposed above sea level or was never developed in this region. The trace fossils reported here provide ichnostratigraphic evidence for a post-Ediacaran age of the Hay Island succession, especially the presence of *Teichichnus*. The earliest *Teichichnus* appear in late Fortunian and Stage 2 rocks, and more generally spreite-burrows have been used as evidence for a post-Ediacaran age in the absence of other evidence (e.g., Bland and Goldring 1995; Jensen *et al.* 2016). *Teichichnus* is a common element in lower Cambrian strata of Avalonia

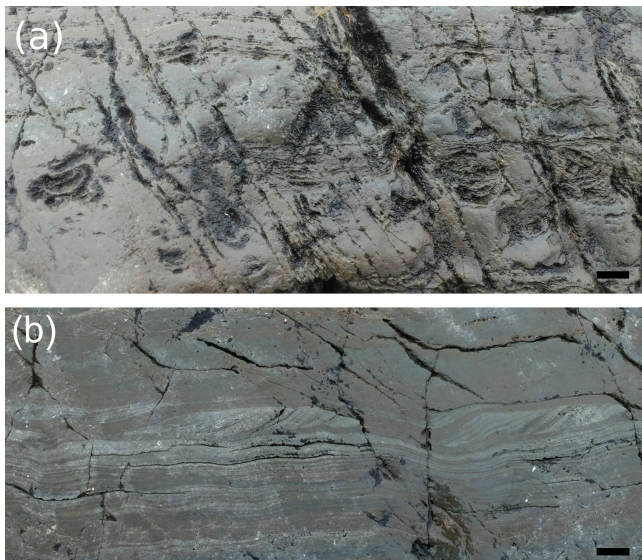


**Figure 7.** Field images of trace fossils and sedimentary structures in the MacCodrum? Formation, southern Hay Island. (a) Siltstone and fine-grained sandstone with transverse sections through *Teichichnus* spreiten. Scale bar represents 10 mm. (b) Current ripple cross-lamination, scale bar represents 10 mm.



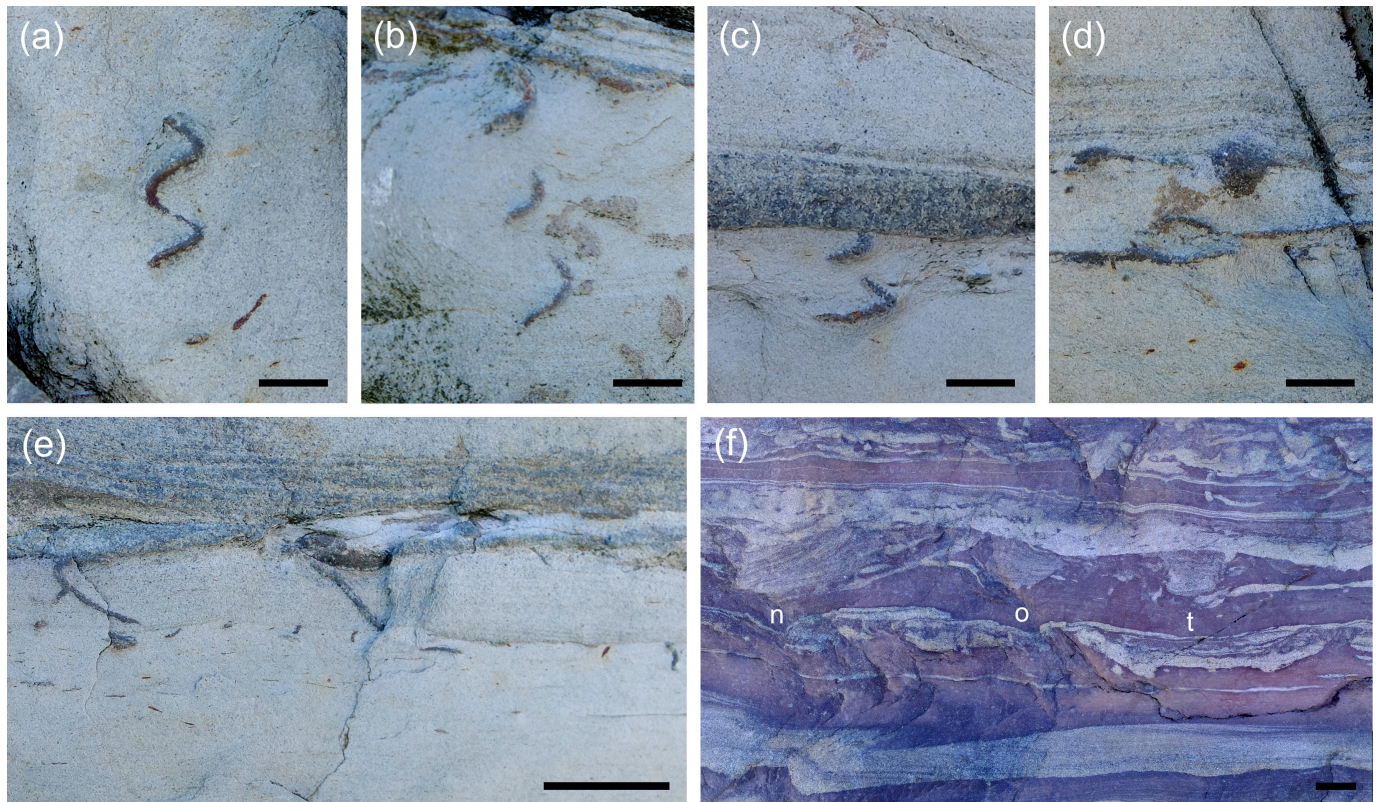


**Figure 8.** Field images of trace fossils from MacCodrum? Formation, northern Hay Island. (a–e) Images from vertical surfaces of cleaved siltstone. (a–c) Vertical spiral trace fossil *Gyrolithes scintillus*. Scale bars represent 5 mm. (d) Small plug-shaped sand-filled structure, which may be a *Conichnus* or a funnel-shaped top of a vertical tube. Scale bar represents 5 mm. (e) Several short trace fossils in “floating” preservation along a bedding plane marked by gentle change in grain size. A larger burrow is a possible *Gyrolithes*. Scale bar represents 5 mm. (f) Vertical view of alternation of sandstone and mudstone in loose block. Along mid-line three discrete *Teichichnus* are seen in, from right to left, transverse (t), oblique (o), and near-longitudinal (n) section. Scale bar represents 5 mm.

and Baltica (Loughlin and Hillier 2010). In the Chapel Island Formation *Teichichnus* occurs sparsely in member 2, more commonly so in members 3 and 4, where it is the dominant trace fossil (Landing *et al.* 1989; Droser *et al.* 2002; Gougeon *et al.* 2018). It is also prominent in the Bonavista Group, in which Landing *et al.* (1989) named a *Teichichnus* Interval. In the Mira River area *Teichichnus* is common in red mudstone of the Canoe Brook Formation (Landing 1991). The earliest *Gyrolithes* straddle the Ediacaran/Cambrian boundary in Newfoundland (Gehling *et al.* 2001; Laing *et al.* 2018), and northern Norway (Jensen *et al.* 2018). Laing *et al.* (2018) documented *Gyrolithes scintillus* from close to the basal Cambrian GSSP through 400 m of section of member 2 of the Chapel Island Formation. If the Hay Island succession overlies that on Scatarie Island, these *Gyrolithes scintillus* are younger than occurrences in Newfoundland.

Finally it is noted that the maximum depositional ages from zircon in the Bengal Road Formation on Scatarie Island are close to the age for the base of the Canoe Brook Formation on Cape Breton Island as inferred from fossils. This suggests that future work is needed to evaluate possible regional differences between the sedimentary successions

on Cape Breton and Scatarie islands. Furthermore, although attribution of the Hay Island succession to the MacCodrum Formation is tentatively maintained here, further studies are needed to confirm this assignment, and to evaluate the possibility that the Hay Island succession is younger than the MacCodrum Formation, and perhaps consistent with the assignment by Barr and White (2017c) to the Miaolingian Trout Brook Formation.

#### ACKNOWLEDGEMENTS

We thank Bruce Hatcher and student assistants from Cape Breton University for transportation by Zodiac to Scatarie Island. We are grateful to Brandon Boucher and Chris McFarlane for assisting Deanne van Rooyen with the U–Pb dating at the University of New Brunswick and for providing invaluable advice in processing and interpreting the age data. We thank Tim Fedak, Nova Scotia Museum of Natural History, for providing collection numbers. Sören Jensen and Teodoro Palacios acknowledge funding from Ministerio de Economía, Industria y Competitividad grant CGL 2017-

87631-P. Sandra Barr acknowledges support from Natural Sciences and Engineering Research Council of Canada Discovery Grant RGPIN-2016-04860. We thank journal reviewers Robert MacNaughton and Andrea Mills for their helpful comments which improved the clarity and readability of the manuscript.

## REFERENCES

- Andersen, T. 2002. Correction of common lead in U–Pb analyses that do not report  $^{204}\text{Pb}$ . *Chemical Geology*, 192, pp.59–79. [https://doi.org/10.1016/S0009-2541\(02\)00195-X](https://doi.org/10.1016/S0009-2541(02)00195-X)
- Archibald, D.B., Barr, S.M., Murphy, J.B., White, C.E., MacHattie, T.G., Escarraga, E.A., Hamilton, M.A., and McFarlane, C.R.M. 2013. Field relationships, petrology, age, and tectonic setting of the Ordovician West Barneys River Plutonic Suite, southern Antigonish Highlands, Nova Scotia, Canada. *Canadian Journal of Earth Sciences*, 50, pp. 727–745. <https://doi.org/10.1139/cjes-2012-0158>
- Barr, S.M. and Raeside, R.P. 1989. Tectono-stratigraphic terranes in Cape Breton Island, Nova Scotia: implications for the configuration of the northern Appalachian orogen. *Geology*, 17, pp. 822–825. [https://doi.org/10.1130/0091-7613\(1989\)017<0822:TSTICB>2.3.CO;2](https://doi.org/10.1130/0091-7613(1989)017<0822:TSTICB>2.3.CO;2)
- Barr, S.M. and White, C.E. 1989. The Main-à-Dieu sequence: an extensive late Precambrian volcanic-sedimentary package in southeastern Cape Breton Island. Nova Scotia Department of Mines and Energy, Report 89-3, pp. 149–152.
- Barr, S.M. and White, C. E. 2017a. Overview map showing locations of bedrock geology maps for Cape Breton Island, Nova Scotia. Nova Scotia Department of Natural Resources, Geoscience and Mines Branch, Open File Map ME 2017-006, scale 1:220 000.
- Barr, S. M. and White, C. E. 2017b. Bedrock geology legend for Cape Breton Island, Nova Scotia; Nova Scotia Department of Natural Resources, Geoscience and Mines Branch, Open File Illustration ME 2017-001.
- Barr, S. M. and White, C. E. 2017c. Bedrock geology map of Glace Bay Area, NTS 11J/04, Cape Breton County, Nova Scotia, Nova Scotia Department of Natural Resources, Geoscience and Mines Branch, Open File Map ME 2017-021, scale 1:50,000.
- Barr, S.M., White, C.E., and Macdonald, A.S. 1992. Revision of upper Precambrian–Cambrian stratigraphy southeastern Cape Breton Island, Nova Scotia; in *Current Research, Part D*; Geological Survey of Canada, Paper 92-1 D, pp. 21–26. <https://doi.org/10.4095/132875>
- Barr, S.M., White, C.E., and Macdonald, A.S. 1996. Stratigraphy, tectonic setting, and geologic history of Late Precambrian volcanic-sedimentary-plutonic belts in southeastern Cape Breton Island, Nova Scotia. *Geological Survey of Canada Bulletin* 468, 84 p. <https://doi.org/10.4095/208235>
- Barr, S.M., Davis, D.W., Kamo, S., and White, C.E. 2003. Significance of U–Pb ages of detrital zircon in quartzite from peri-Gondwanan terranes, New Brunswick and Nova Scotia, Canada. *Precambrian Research*, 126, pp. 123–145. [https://doi.org/10.1016/S0301-9268\(03\)00192-X](https://doi.org/10.1016/S0301-9268(03)00192-X)
- Barr, S.M., Hamilton, M.A., Samson, S.D., Satkoski, A., and White, C.E. 2012. Provenance variations in northern Appalachian Avalonia based on detrital zircon age patterns in Ediacaran and Cambrian sedimentary rocks, New Brunswick and Nova Scotia, Canada. *Canadian Journal of Earth Sciences*, 49, pp. 533–546. <https://doi.org/10.1139/e11-070>
- Bevier, M.L., Barr, S.M., White, C.E., and Macdonald, A.S. 1993. U–Pb geochronologic constraints on the volcanic evolution of the Mira (Avalon) terrane, southeastern Cape Breton Island, Nova Scotia. *Canadian Journal of Earth Sciences*, 30, pp. 1–10. <https://doi.org/10.1139/e93-001>
- Bland, B.H. and Goldring, R. 1995. *Teichichnus* Seilacher 1955 and other trace fossils (Cambrian?) from the Charnian of central England. *Neues Jahrbuch für Geologie und Paläontologie, Abhandlungen*, 195, pp. 5–23. <https://doi.org/10.1127/njgpa/195/1995/5>
- Dickinson, W.R. and Gehrels, G.E. 2010. Insights into North American paleogeography and paleotectonics from U–Pb ages of detrital zircons in Mesozoic strata of the Colorado Plateau, USA. *International Journal of Earth Sciences*, 99, pp. 1247–1265. <https://doi.org/10.1007/s00531-009-0462-0>
- Droser, M.L., Jensen, S., Gehling, J.G., Myrow, P.M., and Narbonne, G.M. 2002. Lowermost Cambrian ichnofabrics from the Chapel Island Formation, Newfoundland: implications for Cambrian substrates. *Palaios*, 17, pp. 3–15. [https://doi.org/10.1669/0883-1351\(2002\)017<0003:L-CIFTC>2.0.CO;2](https://doi.org/10.1669/0883-1351(2002)017<0003:L-CIFTC>2.0.CO;2)
- Fletcher, H. 1879. Report of explorations and surveys in Cape Breton, Nova Scotia. Geological Survey of Canada Report of Progress for 1877–78, Part F, 11, 32 p.
- Gehling, J.G., Jensen, S., Droser, M.L., Myrow, P.M., and Narbonne, G.M. 2001. Burrowing below the basal Cambrian GSSP, Fortune Head, Newfoundland. *Geological Magazine*, 138, pp. 213–218. <https://doi.org/10.1017/S001675680100509X>
- Geyer, G. 2019. A comprehensive Cambrian correlation chart. *Episodes*, 42, pp. 321–332. <https://doi.org/10.18814/epiugs/2019/019026>
- Gougeon, R.C., Mangano, M.G., Buatois, L.A., Narbonne, G.M., and Laing, B.A. 2018. Early Cambrian origin of the shelf sediment mixed layer. *Nature Communications*, 9(1909), 8 p. <https://doi.org/10.1038/s41467-018-04311-8>
- Hayes, A.O., Bell, W.A., and Goranson, E.A. 1938. Glace Bay sheet; Department of Mines and Resources, Map 362A, scale 1:63 360.
- Hibbard, J.P., van Staal, C.R., Rankin, D.W., and Williams, H., 2006. Lithotectonic map of the Appalachian Orogen, Canada-United States of America; Geological Survey



- of Canada, Map 2096A, scale 1:1 500 000. <https://doi.org/10.4095/221912>
- Hutchinson, R.D. 1952. The stratigraphy and trilobite faunas of the Cambrian sedimentary rocks of Cape Breton Island, Nova Scotia; Geological Survey of Canada, Memoir 263, 124 p. <https://doi.org/10.4095/101599>
- Jensen, S., Harper, D.A.T., and Stouge, S. 2016. Trace fossils from the lower Cambrian Kløftelv Formation, Ella Ø, North-East Greenland. *GFF*, 138, pp. 369–376. <https://doi.org/10.1080/11035897.2015.1076029>
- Jensen, S., Högström, A.E.S., Almond, J., Taylor, W.L., Meinhold, G., Høyberget, M., Ebbestad, J.O.R., Agić, H., and Palacios, T. 2018. Scratch circles from the Ediacaran and Cambrian of Arctic Norway and southern Africa, with a review of scratch circle occurrences. *Bulletin of Geosciences*, 93, pp. 287–304. <https://doi.org/10.3140/bull.geosci.1685>
- Laing, B.A., Buatois, L.A., Mángano, M.G., Narbonne, G.M., and Gougeon, R.C. 2018. *Gyrolithes* from the Ediacaran–Cambrian boundary section in Fortune Head, Newfoundland, Canada: exploring the onset of complex burrowing; *Palaeogeography, Palaeoclimatology, Palaeoecology*, 405, pp. 171–185. <https://doi.org/10.1016/j.palaeo.2018.01.010>
- Landing, E. 1991. Upper Precambrian through Lower Cambrian of Cape Breton Island: faunas, paleoenvironments, and stratigraphic revision; *Journal of Paleontology*, 65, pp. 570–595. <https://doi.org/10.1017/S0022336000030675>
- Landing, E. 1996. Avalon: insular continent in the Cambrian. *In* *Avalonian and related peri-Gondwanan terranes of the circum-North Atlantic*. Edited by D. Nance and M.D. Thompson. Geological Society America Special Paper, 304, pp. 29–63. <https://doi.org/10.1130/0-8137-2304-3.29>
- Landing, E. 2004. Precambrian–Cambrian boundary interval deposition and the marginal platform of the Avalon microcontinent. *Journal of Geodynamics*, 37, pp. 411–435. <https://doi.org/10.1016/j.jog.2004.02.014>
- Landing, E., Myrow, P.M., Benus, A.P., and Narbonne, G.M. 1989. The Placentian Series: appearance of the oldest skeletalized faunas in southeastern Newfoundland. *Journal of Paleontology*, 63, pp. 739–769. <https://doi.org/10.1017/S0022336000036465>
- Loughlin, N.J.D. and Hillier, R.D. 2010. Early Cambrian *Teichichnus*-dominated ichnofabrics and palaeoenvironmental analysis of the Caerfai Group, southwest Wales, UK. *Palaeogeography, Palaeoclimatology, Palaeoecology*, 297, 239–251. <https://doi.org/10.1016/j.palaeo.2010.07.030>
- Ludwig, K.R. 2012. Isoplot 4.15: A geochronological toolkit for Microsoft Excel. Berkeley Geochronological Center. URL <[http://www.bgc.org/isoplot\\_etc/isoplot/Isoplot4\\_15files.zip](http://www.bgc.org/isoplot_etc/isoplot/Isoplot4_15files.zip)>, March 2020.
- McFarlane, C.R.M. and Luo, Y. 2012. Modern analytical facilities: U–Pb geochronology using 193 nm Excimer LA-ICP-MS optimized for in-situ accessory mineral dating in thin sections. *Geoscience Canada*, 39(3), pp. 158–172.
- Palacios, T., Jensen, S., Barr, S.M., and White, C.E. 2009. Acritarchs from the MacLean Brook Formation, south-eastern Cape Breton Island, Nova Scotia, Canada: new data on Middle Cambrian–Lower Furongian acritarch zonation. *Palaeogeography, Palaeoclimatology, Palaeoecology*, 273, pp. 123–141. <https://doi.org/10.1016/j.palaeo.2008.12.006>
- Palacios, T., Jensen, S., Barr, S.M., and White, C.E. 2015. Stratigraphic constraints on Cambrian stratigraphy. Mira and Bras d’Or terranes, Cape Breton Island, Nova Scotia, Canada. *Atlantic Geology*, 51, pp. 127–128. <https://doi.org/10.4138/atlgol.2015.005>
- Paton, C., Hellstrom, J., Paul, B., Woodhead, J., and Hergt, J.M. 2011. Iolite: freeware for the visualisation and processing of mass spectrometric data. *Journal of Analytical Atomic Spectrometry*, 26, pp. 2508–2518. <https://doi.org/10.1039/c1ja10172b>
- Petrus, J.A. and Kamber, B.S. 2012. VizualAge: A novel approach to laser ablation ICP-MS U–Pb geochronology data reduction. *Geostandards and Geoanalytical Research*, 36, pp. 247–270. <https://doi.org/10.1111/j.1751-908X.2012.00158.x>
- Reynolds, P.H., Barr, S.M., and White, C.E. 2009. Provenance of detrital muscovite in Cambrian Avalonia of Maritime Canada:  $^{40}\text{Ar}/^{39}\text{Ar}$  ages and chemical compositions. *Canadian Journal of Earth Sciences*, 46, pp. 169–180. <https://doi.org/10.1139/E09-013>
- Sarjeant, W.A.S. and Stancliffe, R.P.W. 1996. The acritarch genus *Polygonium* Vavrdová emend Sarjeant and Stancliffe 1994: a reassessment of its constituent species. *Annales de la Société géologique de Belgique*, 117, pp. 355–369. <https://doi.org/10.2307/1485867>
- van Staal, C.R., Barr, S.M., McCausland, P.M., Thompson, M.D., and White, C.E. 2020. Tonian-Ediacaran tectonomagmatic evolution of West Avalonia and its Ediacaran–Early Cambrian interactions with Ganderia: an example of complex terrane transfer due to arc–arc collision? *In* *Pannotia to Pangaea: Neoproterozoic and Paleozoic orogenic cycles in the circum-Atlantic region*. Edited by J.B. Murphy, R.A. Strachan, and C. Quesada. Geological Society, London, Special Publications, 503. <https://doi.org/10.1144/SP503-2020-23>
- Vidal, G. 1988. A palynological preparation method. *Paly-nology*, 12, pp. 215–220. <https://doi.org/10.1080/01916122.1988.9989345>
- Weeks, F.J. 1954. Southeast Cape Breton Island, Nova Scotia. Geological Survey of Canada, Memoir 277, 112 p. <https://doi.org/10.4095/101500>
- Willner, A.P., Barr, S.M., Gerdes, A., Massonne, H.-J., and White, C.E. 2013. Origin and evolution of Avalonia: evidence from U–Pb and Lu–Hf isotopes in zircon from the Mira terrane, Canada, and the Stavelot–Venn Massif, Belgium. *Journal of the Geological Society, London*, 170, pp. 769–784. <https://doi.org/10.1144/jgs2012-152>

*Editorial responsibility: Robert A. Fensome*

#### APPENDIX A: U–PB DATA TABLES



**Table A1.** LA-ICP-MS U-Pb isotopic analyses of detrital zircon samples analyzed at the University of New Brunswick.

Corrections: 1 = threshold <sup>204</sup>Pb no correction (100 cps); 2 = threshold % <sup>204</sup>Pb-based correction(20% error) ; 3 = threshold % for <sup>208</sup>Pb-based correction (98.5 %Pb\*).

Sample	<sup>90</sup> Zr cps	U (ppm)	Th (ppm)	Th/U	<sup>204</sup> Pb cps	± 2σ	% ±	<sup>206</sup> Pb/ <sup>204</sup> Pb cps	% Pb <sup>2+</sup>	Corrections	Isotopic ratios			Calculated ages											
											<sup>207</sup> Pb/ <sup>235</sup> U ± 2σ	<sup>206</sup> Pb/ <sup>238</sup> U ± 2σ	EC <sup>3</sup>	<sup>207</sup> Pb/± 2σ	<sup>206</sup> Pb/± 2σ	<sup>207</sup> Pb/± 2σ	<sup>206</sup> Pb/± 2σ	% conc							
<b>SMB17-234 Run 1 Grid Zone 21T (WGS84) 290042 5099656</b>																									
SMB17-234 - 1 <sup>a</sup>	1.86E+08	469	266.7	1.76	-9	11	-122.2	120050	99.83	1	FALSE	3.282	0.087	0.256	0.004	0.266	0.0934	0.0013	1496	26	1476	20	1470	21	98.2
SMB17-234 - 2 <sup>a,b</sup>	1.95E+08	210.2	121	1.74	7	14	200.0	2566	99.74	1	FALSE	0.687	0.025	0.086	0.002	0.205	0.0588	0.0018	560	67	530	15	529	10	99.8
SMB17-234 - 3 <sup>a</sup>	1.86E+08	222	206.1	1.08	6	14	233.3	3243	99.69	1	FALSE	0.668	0.027	0.081	0.001	0.486	0.0599	0.0020	600	72	518	17	504	8	97.2
SMB17-234 - 4 <sup>a</sup>	1.85E+08	103	73.6	1.40	14	12	85.7	714	99.74	1	FALSE	0.789	0.033	0.097	0.002	0.271	0.0598	0.0021	596	76	587	19	594	11	101.2
SMB17-234 - 5 <sup>a</sup>	2.01E+08	427.1	101	4.23	4	15	375.0	30050	99.74	1	FALSE	3.569	0.092	0.267	0.004	0.458	0.0978	0.0013	1583	25	1542	21	1526	21	96.4
SMB17-234 - 6 <sup>a</sup>	1.85E+08	122.2	60.8	2.01	1	11	1100.0	10560	99.75	1	FALSE	0.683	0.032	0.086	0.002	0.070	0.0583	0.0025	541	94	525	20	531	9	101.2
SMB17-234 - 7	2.13E+08	207.7	67.7	3.07	16	17	106.3	2624	98.38	1	FALSE	2.438	0.098	0.193	0.004	0.464	0.0917	0.0028	1461	58	1251	29	1139	22	78.0
SMB17-234 - 8 <sup>a</sup>	1.77E+08	111.7	70.9	1.58	-5	12	-240.0	38810	99.72	1	FALSE	5.738	0.160	0.350	0.006	0.480	0.1201	0.0022	1958	33	1935	25	1931	29	98.6
SMB17-234 - 9	1.78E+08	459	84.2	5.45	1	16	1600.0	101000	98.13	1	FALSE	3.022	0.085	0.221	0.004	0.569	0.1000	0.0016	1624	30	1412	21	1287	19	79.2
SMB17-234 - 10 <sup>a</sup>	1.68E+08	268.2	37.66	7.12	5	11	220.0	5146	99.87	1	FALSE	0.883	0.027	0.105	0.002	0.113	0.0614	0.0014	653	49	641	15	645	10	100.7
SMB17-234 - 11 <sup>a,b</sup>	1.84E+08	109.5	119	0.92	-1	13	-1300.0	9500	99.53	1	FALSE	0.688	0.032	0.085	0.002	0.238	0.0595	0.0024	585	88	531	20	524	10	98.7
SMB17-234 - 12 <sup>a</sup>	1.89E+08	101.3	86.64	1.17	-5	13	-260.0	31580	99.52	1	FALSE	4.435	0.130	0.302	0.005	0.393	0.1078	0.0021	1763	36	1717	24	1698	26	96.3
SMB17-234 - 13	2.19E+08	547	34.73	15.75	4	21	525.0	22375	99.57	1	FALSE	1.636	0.081	0.159	0.005	0.871	0.0753	0.0019	1077	51	981	30	951	27	88.3
SMB17-234 - 14 <sup>a,b</sup>	1.78E+08	274	165	1.66	8	14	175.0	2785	99.74	1	FALSE	0.668	0.023	0.084	0.002	0.175	0.0583	0.0017	541	64	520	14	520	9	100.0
SMB17-234 - 15 <sup>a,b</sup>	1.76E+08	113.1	54.1	2.09	3	10	346.4	3243	99.63	1	FALSE	0.683	0.028	0.085	0.002	0.226	0.0592	0.0020	574	73	526	17	524	9	99.6
SMB17-234 - 16 <sup>a</sup>	1.90E+08	108.6	60	1.81	-3	13	-433.3	9810	99.81	1	FALSE	0.710	0.035	0.090	0.002	0.159	0.0578	0.0026	522	99	545	20	555	11	101.8
SMB17-234 - 17 <sup>a</sup>	1.87E+08	164.6	90.9	1.81	3	10	333.3	4803	99.89	1	FALSE	0.674	0.028	0.086	0.002	0.036	0.0574	0.0019	507	73	521	17	531	9	101.8
SMB17-234 - 18 <sup>a</sup>	1.82E+08	241.5	145.1	1.66	-6	12	-200.0	19870	99.72	1	FALSE	0.661	0.023	0.083	0.001	0.198	0.0585	0.0016	549	60	516	13	512	8	99.3
SMB17-234 - 20 <sup>a,b</sup>	1.85E+08	134.8	79.6	1.69	1	11	1100.0	11490	99.61	1	FALSE	0.679	0.025	0.084	0.002	0.142	0.0591	0.0018	571	66	524	15	520	9	99.3
SMB17-234 - 21 <sup>a</sup>	1.69E+08	175.4	91.25	1.92	9	15	166.7	5514	99.69	1	FALSE	4.004	0.120	0.285	0.005	0.428	0.1024	0.0019	1668	34	1634	24	1618	24	97.0
SMB17-234 - 22	1.96E+08	168.7	127.3	1.33	6	11	183.3	8210	98.74	1	FALSE	4.020	0.110	0.272	0.004	0.543	0.1076	0.0018	1759	31	1636	23	1552	22	88.2
SMB17-234 - 23 <sup>a</sup>	1.84E+08	152.6	72.3	2.11	4	12	300.0	3120	99.57	1	FALSE	0.662	0.028	0.080	0.002	0.225	0.0605	0.0022	622	78	513	17	496	9	96.6
SMB17-234 - 24 <sup>a</sup>	1.90E+08	209.7	182.9	1.15	5	13	260.0	3690	99.80	1	FALSE	0.690	0.024	0.087	0.002	0.153	0.0580	0.0017	530	64	532	14	537	9	100.9
SMB17-234 - 25 <sup>a,b</sup>	1.75E+08	134	114	1.18	8	11	137.5	1349	99.85	1	FALSE	0.668	0.031	0.084	0.002	0.270	0.0576	0.0020	515	76	519	18	520	9	100.2
SMB17-234 - 26 <sup>a</sup>	1.92E+08	818	13.1	62.44	1	13	1300.0	85700	99.82	1	FALSE	0.852	0.025	0.103	0.002	0.399	0.0609	0.0012	634	42	625	14	629	10	100.6
SMB17-234 - 27 <sup>a</sup>	1.90E+08	96.7	103.6	0.93	4	14	350.0	2445	99.68	1	FALSE	0.856	0.039	0.102	0.002	0.135	0.0609	0.0025	636	88	625	21	629	11	100.6
SMB17-234 - 28	1.76E+08	1237	238.8	5.18	31	13	41.9	5548	98.89	1	FALSE	1.564	0.043	0.146	0.003	0.777	0.0776	0.0010	1136	26	955	17	881	14	77.5
SMB17-234 - 29 <sup>a</sup>	2.05E+08	195.7	184	1.06	3	15	500.0	6080	99.75	1	FALSE	0.725	0.033	0.090	0.002	0.080	0.0586	0.0025	552	93	552	19	554	10	100.4
SMB17-234 - 30 <sup>a</sup>	1.62E+08	757	590	1.28	9	15	166.7	6233	99.51	1	FALSE	0.639	0.022	0.077	0.002	0.540	0.0604	0.0014	618	50	501	13	478	9	95.5
SMB17-234 - 31 <sup>a,b</sup>	1.94E+08	188	87.6	2.15	8	19	237.5	2071	99.71	1	FALSE	0.686	0.032	0.085	0.002	0.082	0.0589	0.0025	563	92	528	19	523	10	99.1
SMB17-234 - 32 <sup>a</sup>	1.94E+08	322	148.5	2.17	3	19	633.3	9063	99.58	1	FALSE	0.678	0.030	0.081	0.002	0.128	0.0606	0.0024	625	85	524	18	502	9	95.9
SMB17-234 - 33 <sup>a</sup>	1.91E+08	188.8	85.6	2.21	2	12	600.0	7975	99.62	1	FALSE	0.682	0.028	0.084	0.001	0.207	0.0591	0.0021	571	77	526	17	519	9	98.7
SMB17-234 - 34 <sup>a</sup>	1.83E+08	620	32.5	19.08	6	11	183.3	13117	99.89	1	FALSE	1.144	0.032	0.127	0.002	0.627	0.0655	0.0010	789	32	774	15	769	12	97.4
SMB17-234 - 35	2.18E+08	446	32.1	13.89	1	18	1800.0	60940	99.35	1	FALSE	1.298	0.049	0.133	0.003	0.694	0.0711	0.0016	960	46	848	19	805	17	83.8

**Table A1.** Continued.

Corrections: 1 = threshold <sup>204</sup>Pb no correction (100 cps); 2 = threshold % <sup>204</sup>Pb-based correction (20% error) ; 3 = threshold % for <sup>208</sup>Pb-based correction (98.5 %Pb\*).

Sample	<sup>90</sup> Zr cps	U (ppm)	Th (ppm)	Th/U	<sup>204</sup> Pb cps <sup>1</sup>	<sup>204</sup> Pb cps ± 2σ	% ± <sup>204</sup> Pb cps	<sup>206</sup> Pb cps	<sup>206</sup> Pb/ <sup>204</sup> Pb %	Corrections	Isotopic ratios			Calculated ages													
											<sup>207</sup> Pb/ <sup>235</sup> U ± 2σ	<sup>206</sup> Pb/ <sup>238</sup> U ± 2σ	EC <sup>3</sup>	<sup>207</sup> Pb/ <sup>206</sup> Pb ± 2σ	<sup>207</sup> Pb/ <sup>235</sup> U ± 2σ	<sup>206</sup> Pb/ <sup>238</sup> U ± 2σ	% conc										
SMB17-234 - 35a <sup>1</sup>	1.50E+08	216.5	50.8	4.26	-6	19	-316.7	40100	99.67	1	FALSE	2.235	0.086	0.200	0.005	0.549	0.0811	0.0025	1224	61	1190	26	1175	27	96.0		
SMB17-234 - 36a	2.23E+08	1601	21.7	73.78	7	36	514.3	26900	99.69	1	FALSE	1.025	0.038	0.114	0.003	0.378	0.0651	0.0019	778	61	716	19	698	15	97.5		
SMB17-234 - 36a <sup>1</sup>	1.56E+08	170.2	48.1	3.54	-15	13	-86.7	51500	99.95	1	FALSE	4.812	0.150	0.322	0.006	0.315	0.1081	0.0024	1768	41	1785	25	1799	29	101.8		
SMB17-234 - 37 <sup>a</sup>	1.83E+08	132.9	93.8	1.42	3	13	433.3	3903	99.66	1	FALSE	0.733	0.033	0.090	0.002	0.407	0.0591	0.0021	571	77	555	19	554	10	99.8		
SMB17-234 - 38	1.81E+08	124.3	72.7	1.71	5	10	200.0	9120	99.99	1	FALSE	6.076	0.170	0.366	0.006	0.535	0.1203	0.0020	1961	30	1985	24	2010	29	102.5		
SMB17-234 - 39	1.57E+08	460	85	5.41	66	28	42.4	574	98.64	1	FALSE	1.111	0.053	0.111	0.003	0.240	0.0729	0.0032	1011	89	758	25	676	18	89.2		
SMB17-234 - 40	2.21E+08	892	28.19	31.64	15	26	173.3	6460	98.64	1	FALSE	1.069	0.037	0.107	0.002	0.586	0.0723	0.0017	994	48	738	19	656	13	88.9		
SMB17-234 - 41 <sup>a</sup>	1.78E+08	181	155	1.17	1	12	1200.0	17300	99.68	1	FALSE	0.782	0.030	0.094	0.002	0.170	0.0596	0.0019	589	69	584	17	582	10	99.6		
SMB17-234 - 42	1.40E+08	624	211	2.96	-2	16	-800.0	135000	97.46	1	FALSE	3.806	0.110	0.248	0.005	0.670	0.1108	0.0019	1813	31	1593	23	1428	24	78.8		
SMB17-234 - 43	1.55E+08	1114	1020	1.09	26	15	57.7	2854	98.99	1	FALSE	0.639	0.019	0.072	0.001	0.300	0.0636	0.0012	728	40	502	12	451	7	89.9		
SMB17-234 - 44 <sup>a</sup>	1.87E+08	227.6	131	1.74	16	16	100.0	1174	99.12	1	FALSE	0.668	0.026	0.076	0.001	0.034	0.0629	0.0021	705	71	518	16	475	8	91.7		
SMB17-234 - 45 <sup>a</sup>	1.81E+08	175.6	104.9	1.67	4	10	250.0	3625	99.60	1	FALSE	0.702	0.024	0.084	0.002	0.328	0.0600	0.0016	604	58	538	14	522	9	97.1		
SMB17-234 - 46	1.50E+08	38.8	5.92	6.55	-3	18	-600.0	8540	99.73	1	FALSE	2.980	0.190	0.248	0.009	0.352	0.0866	0.0050	1352	111	1390	49	1429	45	105.7		
SMB17-234 - 47 <sup>ab</sup>	1.80E+08	56.6	118.4	0.48	13	11	84.6	362	99.69	1	FALSE	0.701	0.042	0.086	0.002	0.156	0.0591	0.0033	571	121	533	25	529	11	99.3		
SMB17-234 - 48	1.95E+08	335	38.2	8.77	13	14	107.7	3600	98.85	1	FALSE	1.436	0.051	0.138	0.004	0.674	0.0754	0.0017	1079	45	902	21	830	20	76.9		
<b>SMB17-234 Run 2 (in italics to distinguish from Run 1)</b>																											
SMB17-234 - 1	2.52E+08	813	147.8	5.50	-1	28	-2800.0	156700	98.02	1	FALSE	1.669	0.036	0.144	0.003	0.719	0.0839	0.0014	1290	32	996	14	870	14	67.4		
SMB17-234 - 2 <sup>a</sup>	1.44E+08	240.9	148.4	1.62	5	13	260.0	3570	99.28	1	FALSE	0.699	0.020	0.082	0.001	0.225	0.0619	0.0017	671	59	537	12	505	8	94.0		
SMB17-234 - 3	2.29E+08	462	81.3	5.68	35	19	54.3	3323	98.33	1	FALSE	2.479	0.045	0.197	0.003	0.763	0.0919	0.0014	1465	29	1265	13	1159	17	79.1		
SMB17-234 - 4 <sup>a</sup>	2.10E+08	145.7	82.7	1.76	-9	15	-166.7	17090	99.56	1	FALSE	0.720	0.028	0.088	0.001	0.025	0.0591	0.0024	571	88	549	16	543	7	98.9		
SMB17-234 - 5	2.13E+08	720	157	4.59	98	22	22.4	2929	97.61	1	FALSE	5.117	0.060	0.300	0.004	0.573	0.1228	0.0010	1997	14	1839	10	1692	18	84.7		
SMB17-234 - 6 <sup>a</sup>	2.44E+08	1361	29.8	45.67	70	25	35.7	2820	99.27	1	FALSE	1.009	0.016	0.108	0.001	0.247	0.0674	0.0009	851	28	708	8	663	8	93.7		
SMB17-234 - 7 <sup>a</sup>	2.15E+08	1912	198	9.66	213	39	18.3	1047	97.64	-	3	0.801	0.041	0.091	0.001	0.335	0.0637	0.0025	732	83	595	24	559	7	93.9		
SMB17-234 - 8 <sup>a</sup>	2.08E+08	352.1	17.2	20.47	13	15	115.4	12708	99.36	1	FALSE	6.411	0.083	0.360	0.004	0.660	0.1281	0.0010	2072	13	2033	11	1983	20	95.7		
SMB17-234 - 9 <sup>a</sup>	2.15E+08	871	43.5	20.02	7	12	171.4	16657	99.58	1	FALSE	0.867	0.014	0.100	0.001	0.716	0.0626	0.0009	694	29	634	8	612	7	96.7		
SMB17-234 - 10	2.21E+08	266	128.7	2.07	5	17	340.0	24280	91.11	1	FALSE	10.530	0.170	0.376	0.006	0.721	0.2030	0.0019	2850	15	2482	15	2057	26	72.2		
SMB17-234 - 11	2.37E+08	543	48.71	11.15	35	17	48.6	2820	99.17	1	FALSE	1.414	0.030	0.139	0.002	0.197	0.0735	0.0015	1028	41	894	13	841	11	81.9		
SMB17-234 - 12 <sup>a</sup>	2.02E+08	254.1	129.9	1.96	3	16	533.3	8760	99.25	1	FALSE	0.670	0.023	0.078	0.001	0.004	0.0616	0.0021	660	73	520	14	486	7	93.4		
SMB17-234 - 13	2.38E+08	805	190.5	4.23	22	15	68.2	9945	98.56	1	FALSE	2.539	0.035	0.202	0.002	0.544	0.0912	0.0008	1450	16	1283	10	1184	13	81.6		
SMB17-234 - 14	1.86E+08	339.9	73.1	4.65	10	17	170.0	6182	98.36	1	FALSE	1.727	0.040	0.151	0.002	0.449	0.0819	0.0016	1243	38	1017	15	907	14	73.0		
SMB17-234 - 15 <sup>a</sup>	2.16E+08	416	299.2	1.39	11	11	100.0	4100	99.19	1	FALSE	0.730	0.015	0.083	0.001	0.100	0.0633	0.0011	718	37	556	9	515	7	92.7		
SMB17-234 - 16 <sup>a</sup>	2.21E+08	292	156	1.87	9	13	144.4	3533	99.21	1	FALSE	0.757	0.020	0.086	0.001	0.017	0.0636	0.0017	728	57	572	11	533	6	93.1		
SMB17-234 - 17 <sup>a</sup>	2.00E+08	308.1	185	1.67	10	19	190.0	3222	99.60	1	FALSE	0.641	0.021	0.080	0.001	0.109	0.0575	0.0019	511	73	502	13	497	7	99.0		
SMB17-234 - 18 <sup>a</sup>	2.48E+08	1297	42.4	30.59	31	27	87.1	5845	99.43	1	FALSE	0.996	0.025	0.109	0.002	0.511	0.0664	0.0013	819	41	701	13	668	9	95.2		
SMB17-234 - 19	2.19E+08	162.1	74.4	2.18	18	12	66.7	1017	98.76	1	FALSE	0.792	0.023	0.085	0.001	0.306	0.0670	0.0018	838	56	591	13	527	7	89.2		
SMB17-234 - 20	2.05E+08	2230	763	2.92	70	15	21.4	6543	98.72	1	FALSE	1.812	0.023	0.161	0.002	0.817	0.0810	0.0005	1221	11	1049	8	963	12	78.9		

Table A1. Continued.

Corrections: 1 = threshold <sup>204</sup>Pb no correction (100 cps); 2 = threshold % <sup>204</sup>Pb-based correction(20% error) ; 3 = threshold % for <sup>208</sup>Pb-based correction (98.5 %Pb\*).

Sample	<sup>90</sup> Zr cps	U (ppm)	Th (ppm)	Th/U	<sup>204</sup> Pb cps <sup>1</sup>	<sup>204</sup> Pb cps ± 2σ	% ± <sup>206</sup> Pb/ <sup>204</sup> Pb	cps	<sup>206</sup> Pb/ <sup>204</sup> Pb %	Pb* <sup>2</sup>	Corrections	Isotopic ratios			Calculated ages										
												<sup>207</sup> Pb/ <sup>235</sup> U ± 2σ	<sup>206</sup> Pb/ <sup>238</sup> U ± 2σ	EC <sup>3</sup>	<sup>207</sup> Pb/ <sup>206</sup> Pb ± 2σ	<sup>207</sup> Pb/ ± 2σ	<sup>206</sup> Pb/ ± 2σ	<sup>207</sup> Pb/ ± 2σ	<sup>206</sup> Pb/ ± 2σ	<sup>207</sup> Pb/ ± 2σ	<sup>206</sup> Pb/ ± 2σ				
SMB17-234-21 <sup>a</sup>	1.35E+08	1856	1321	1.40	151	29	19.2	897	97.79	-	3	0.660	0.045	0.082	0.001	0.443	0.0580	0.0035	530	132	511	28	506	7	98.9
SMB17-234-22 <sup>a</sup>	1.94E+08	270.4	160.9	1.68	1	15	1500.0	26700	98.97	1	FALSE	0.696	0.024	0.078	0.001	0.325	0.0639	0.0021	738	70	535	14	487	7	91.0
SMB17-234-23	2.17E+08	254	155.9	1.63	9	11	122.2	3124	98.89	1	FALSE	0.749	0.017	0.082	0.001	0.417	0.0658	0.0013	800	41	567	10	508	7	89.7
SMB17-234-24	2.03E+08	598.1	168	3.56	14	15	107.1	11743	98.82	1	FALSE	2.638	0.038	0.210	0.003	0.236	0.0904	0.0009	1433	19	1311	11	1229	14	85.8
SMB17-234-25	1.97E+08	986	116	8.50	21	14	66.7	14571	97.52	1	FALSE	3.829	0.046	0.250	0.003	0.709	0.1103	0.0008	1804	13	1598	10	1436	16	79.6
SMB17-234-26	2.19E+08	1130	248	4.56	97	21	21.6	1344	97.46	1	FALSE	0.957	0.024	0.088	0.002	0.673	0.0780	0.0013	1147	33	681	12	545	12	84.0
SMB17-234-27	1.97E+08	925	147.9	6.25	2	14	700.0	115300	98.83	1	FALSE	2.447	0.039	0.200	0.003	0.770	0.0881	0.0008	1384	17	1256	12	1175	15	80.9
SMB17-234-28	1.56E+08	1284	476	2.70	94	33	35.1	3768	97.89	1	FALSE	4.180	0.058	0.269	0.003	0.449	0.1119	0.0012	1831	19	1670	11	1533	17	83.7
SMB17-234-29 <sup>a</sup>	2.00E+08	362.8	79.3	4.58	11	13	118.2	9373	99.37	1	FALSE	2.784	0.049	0.225	0.003	0.606	0.0892	0.0011	1408	24	1350	13	1307	17	92.8
SMB17-234-30 <sup>a,b</sup>	2.23E+08	246.6	167.8	1.47	-4	14	-350.0	27270	99.65	1	FALSE	0.700	0.020	0.086	0.001	0.212	0.0590	0.0017	567	63	538	12	531	8	98.6
SMB17-234-31 <sup>a,b</sup>	2.41E+08	316.9	201.7	1.57	-1	20	-2000.0	36090	99.63	1	FALSE	0.687	0.018	0.084	0.001	0.005	0.0592	0.0016	574	59	530	11	521	7	98.3
SMB17-234-32 <sup>a</sup>	1.99E+08	152.5	13.15	11.60	1	15	1500.0	24200	99.54	1	FALSE	1.174	0.031	0.129	0.002	0.252	0.0659	0.0016	803	51	787	14	780	11	97.1
SMB17-234-33	1.88E+08	218.4	94.9	2.30	12	17	141.7	6342	97.87	1	FALSE	4.612	0.084	0.285	0.005	0.638	0.1166	0.0015	1905	23	1750	15	1615	23	84.8
SMB17-234-34	2.15E+08	406	225	1.80	2	10	500.0	66100	98.28	1	FALSE	3.381	0.045	0.239	0.003	0.545	0.1017	0.0010	1656	18	1499	10	1383	16	83.5
SMB17-234-35	2.47E+08	965	44	21.93	215	31	14.4	1774	96.17	-	3	5.209	0.087	0.295	0.004	0.670	0.1281	0.0013	2072	18	1854	14	1665	19	80.4
SMB17-234-36	2.48E+08	778	32.8	23.72	6	28	466.7	23500	99.46	1	FALSE	1.325	0.085	0.136	0.005	0.957	0.0708	0.0022	952	64	853	36	819	27	86.1
SMB17-234-37 <sup>a</sup>	2.25E+08	399	127	3.14	-2	13	-650.0	175600	98.77	1	FALSE	5.867	0.067	0.337	0.004	0.564	0.1258	0.0009	2040	12	1956	10	1874	19	91.9
SMB17-234-38	2.00E+08	423	109.1	3.88	71	19	26.8	2146	97.04	1	FALSE	4.740	0.069	0.279	0.004	0.633	0.1222	0.0011	1989	16	1774	12	1587	18	79.8
SMB17-234-39 <sup>a</sup>	2.13E+08	59.9	53.88	1.11	8	11	137.5	3304	99.21	1	FALSE	5.950	0.110	0.349	0.005	0.487	0.1235	0.0018	2007	26	1965	16	1928	23	96.0
SMB17-234-40 <sup>a</sup>	2.03E+08	161.8	98.3	1.65	12	13	108.3	1429	99.18	1	FALSE	0.731	0.022	0.084	0.001	0.094	0.0633	0.0020	718	67	558	13	520	8	93.2
SMB17-234-41	2.02E+08	644.6	555	1.16	6	18	300.0	42733	98.20	1	FALSE	5.144	0.065	0.308	0.004	0.413	0.1207	0.0011	1967	16	1843	11	1729	18	87.9
SMB17-234-42 <sup>a</sup>	2.13E+08	142.6	97.8	1.46	10	13	130.0	1566	98.89	1	FALSE	0.734	0.025	0.082	0.001	0.442	0.0651	0.0019	778	61	557	15	507	8	91.0
SMB17-234-43 <sup>a</sup>	2.13E+08	172.3	90.7	1.90	3	11	366.7	15570	99.24	1	FALSE	2.543	0.040	0.211	0.003	0.398	0.0876	0.0013	1374	29	1283	12	1236	14	90.0
SMB17-234-44 <sup>a</sup>	2.11E+08	149.2	105.9	1.41	8	11	137.5	8850	99.78	1	FALSE	6.540	0.090	0.374	0.005	0.544	0.1268	0.0012	2054	17	2050	12	2047	21	99.7
SMB17-234-45 <sup>a</sup>	2.14E+08	182.2	98.3	1.85	1	12	1200.0	19070	99.38	1	FALSE	0.684	0.019	0.081	0.001	0.047	0.0607	0.0016	629	57	528	11	505	6	95.5
SMB17-234-46 <sup>a</sup>	2.17E+08	1280	31	41.29	16	10	62.4	10580	99.75	1	FALSE	0.826	0.011	0.098	0.001	0.427	0.0614	0.0006	653	21	611	6	601	7	98.3
SMB17-234-47	2.22E+08	491	126.4	3.88	22	13	59.1	7423	97.79	1	FALSE	3.747	0.043	0.250	0.003	0.550	0.1089	0.0007	1782	12	1581	9	1436	15	80.6
SMB17-234-48	2.31E+08	690.4	48.2	14.32	35	25	71.4	3580	97.91	1	FALSE	1.721	0.056	0.146	0.003	0.907	0.0858	0.0014	1334	32	1015	21	880	17	66.0
SMB17-234-49 <sup>a</sup>	2.23E+08	314.1	149.8	2.10	7	13	185.7	4967	99.72	1	FALSE	0.697	0.014	0.086	0.001	0.223	0.0588	0.0011	560	41	537	8	533	7	99.3
SMB17-234-50	1.99E+08	135.7	53.6	2.53	12	12	100.0	3246	97.76	1	FALSE	3.358	0.065	0.232	0.004	0.561	0.1048	0.0015	1711	26	1493	15	1347	18	78.7
SMB17-234-51	2.18E+08	189.9	109.1	1.74	25	12	48.0	815	98.78	1	FALSE	0.758	0.018	0.083	0.001	0.129	0.0668	0.0015	832	47	572	10	511	6	89.4
SMB17-234-52	2.45E+08	773	118.9	6.50	33	25	75.8	3645	98.40	1	FALSE	1.245	0.034	0.119	0.002	0.588	0.0768	0.0016	1116	42	821	15	722	11	87.9
SMB17-234-53 <sup>a,b</sup>	2.14E+08	196.2	107.6	1.82	7	11	157.1	3050	99.64	1	FALSE	0.690	0.019	0.086	0.001	0.279	0.0584	0.0015	545	56	532	11	531	7	99.9
SMB17-234-54 <sup>a</sup>	2.05E+08	696	47.6	14.62	37	22	59.5	2381	99.26	1	FALSE	1.128	0.037	0.118	0.002	0.598	0.0698	0.0018	922	53	766	18	720	12	94.0
SMB17-234-55 <sup>a</sup>	2.13E+08	687.1	98.1	7.00	12	15	125.0	20008	99.26	1	FALSE	3.629	0.053	0.262	0.003	0.601	0.1004	0.0010	1631	18	1555	12	1502	16	92.1
SMB17-234-56	2.08E+08	415.8	243.6	1.71	9	15	166.7	12722	98.52	1	FALSE	2.737	0.040	0.212	0.003	0.589	0.0940	0.0010	1508	20	1338	11	1239	16	82.2

Table A1. Continued.

Corrections: 1 = threshold <sup>204</sup>Pb no correction (100 cps); 2 = threshold % <sup>204</sup>Pb-based correction (20% error) ; 3 = threshold % for <sup>208</sup>Pb-based correction (98.5 %Pb\*).

Sample	<sup>90</sup> Zr cps	U (ppm)	Th (ppm)	Th/U	<sup>204</sup> Pb cps <sup>1</sup>	<sup>204</sup> Pb cps ± 2σ	% ± <sup>206</sup> Pb/ <sup>204</sup> Pb	cps	<sup>206</sup> Pb/ <sup>204</sup> Pb %	Corrections		Isotopic ratios				Calculated ages									
										1	2	<sup>207</sup> Pb/ <sup>235</sup> U ± 2σ	<sup>206</sup> Pb/ <sup>238</sup> U ± 2σ	EC <sup>3</sup>	<sup>207</sup> Pb/ <sup>206</sup> Pb ± 2σ	<sup>207</sup> Pb/ ± 2σ	<sup>206</sup> Pb/ ± 2σ	<sup>207</sup> Pb/ ± 2σ	<sup>206</sup> Pb/ ± 2σ						
SMB17-234-57	2.17E+08	382.7	137.8	2.78	56	16	28.6	2825	97.69	1	FALSE	5.233	0.084	0.306	0.004	0.811	0.1248	0.0011	2026	16	1859	15	1720	22	84.9
SMB17-234-58 <sup>d</sup>	2.04E+08	209.7	118.4	1.77	6	12	200.0	3578	99.15	1	FALSE	0.681	0.019	0.078	0.001	0.156	0.0629	0.0017	705	58	526	11	487	7	92.6
SMB17-234-59 <sup>d</sup>	2.20E+08	625	596	1.05	21	12	57.1	2919	99.36	1	FALSE	0.638	0.011	0.076	0.001	0.408	0.0616	0.0008	659	28	501	7	470	6	93.8
SMB17-234-60	2.10E+08	388.8	150.9	2.58	36	15	41.7	3575	94.59	1	FALSE	4.831	0.100	0.256	0.005	0.819	0.1373	0.0016	2193	20	1788	19	1467	27	66.9
SMB17-234-61 <sup>d</sup>	1.96E+08	162.8	94.5	1.72	8	17	212.5	2066	99.48	1	FALSE	0.632	0.029	0.078	0.002	0.022	0.0587	0.0028	556	104	496	18	486	10	97.9
SMB17-234-62 <sup>d</sup>	2.46E+08	814	20.9	38.95	18	20	111.1	6350	99.49	1	FALSE	0.917	0.021	0.103	0.001	0.227	0.0653	0.0016	784	51	663	12	633	8	95.5
SMB17-234-63	2.46E+08	477.9	439.7	1.09	33	19	57.6	7045	95.52	1	FALSE	7.760	0.160	0.356	0.005	0.764	0.1595	0.0020	2450	21	2201	19	1962	22	80.1
SMB17-234-64	2.59E+08	843.4	87.4	9.65	1	23	2300.0	390300	95.86	1	FALSE	6.923	0.110	0.336	0.005	0.690	0.1508	0.0015	2355	17	2101	14	1868	24	79.3
SMB17-234-65 <sup>d</sup>	2.21E+08	510	219	2.33	-1	10	-1000.0	163200	99.51	1	FALSE	3.110	0.044	0.243	0.003	0.756	0.0932	0.0007	1492	14	1434	11	1402	17	94.0
SMB17-234-66 <sup>d</sup>	1.96E+08	156	97.6	1.60	6	14	233.3	3527	99.16	1	FALSE	1.020	0.036	0.109	0.002	0.148	0.0675	0.0022	853	68	711	18	668	10	93.9
SMB17-234-67	2.11E+08	525	80.5	6.52	6	10	166.7	13583	98.14	1	FALSE	1.348	0.021	0.123	0.002	0.455	0.0795	0.0010	1184	24	866	9	751	9	63.4
SMB17-234-69	2.44E+08	1631	765	2.13	65	21	32.3	5858	97.19	1	FALSE	2.223	0.035	0.169	0.002	0.736	0.0961	0.0008	1549	16	1188	11	1006	13	64.9
SMB17-234-70	2.18E+08	1136	109.3	10.39	3	13	433.3	89100	98.87	1	FALSE	2.343	0.028	0.194	0.002	0.525	0.0881	0.0007	1384	15	1225	9	1145	13	82.8
SMB17-234-71 <sup>d</sup>	2.20E+08	602	32.3	18.64	29	16	55.2	3052	98.90	1	FALSE	1.126	0.026	0.114	0.002	0.445	0.0717	0.0014	977	40	765	13	698	9	91.2
SMB17-234-72	2.12E+08	299.6	82	3.65	5	12	240.0	8940	98.51	1	FALSE	1.188	0.029	0.115	0.002	0.480	0.0749	0.0014	1066	38	794	13	702	9	88.4
SMB17-234-73	1.94E+08	944	200.3	4.71	36	15	41.7	9000	98.77	1	FALSE	4.174	0.049	0.279	0.003	0.700	0.1087	0.0017	1777	11	1669	10	1586	17	89.2
SMB17-234-74	2.30E+08	270.1	70.8	3.81	19	15	78.9	2253	97.79	1	FALSE	1.379	0.035	0.122	0.002	0.300	0.0824	0.0019	1255	45	879	15	744	10	84.6
SMB17-234-75	1.84E+08	751	31.3	23.99	64	16	25.0	1630	98.57	1	FALSE	1.315	0.018	0.126	0.002	0.412	0.0763	0.0008	1103	22	853	8	762	10	69.1
SMB17-234-76 <sup>d</sup>	2.04E+08	300	91.4	3.28	6	13	216.7	20533	98.62	1	FALSE	5.158	0.082	0.313	0.005	0.735	0.1195	0.0011	1949	16	1845	14	1756	24	90.1
SMB17-234-77 <sup>d</sup>	2.13E+08	163.4	102.1	1.60	3	10	333.3	5850	99.47	1	FALSE	0.703	0.021	0.085	0.001	0.385	0.0599	0.0016	600	58	538	12	527	7	97.9
SMB17-234-78 <sup>d</sup>	1.52E+08	223.9	190.8	1.17	6	17	283.3	2963	99.22	1	FALSE	0.735	0.024	0.084	0.001	0.194	0.0633	0.0020	718	67	558	14	522	9	93.6
SMB17-234-79 <sup>ab</sup>	2.13E+08	224.1	131.7	1.70	-6	10	-176.4	24200	99.57	1	FALSE	0.695	0.016	0.085	0.001	0.044	0.0595	0.0014	585	51	535	10	526	6	98.5
SMB17-234-80	1.93E+08	186.2	152.3	1.22	-4	10	-250.0	55100	99.85	1	FALSE	2.905	0.049	0.242	0.003	0.329	0.0868	0.0013	1356	29	1382	13	1397	17	103.0
SMB17-234-81 <sup>d</sup>	2.34E+08	135	88	1.53	11	13	118.2	9018	98.56	1	FALSE	16.580	0.220	0.553	0.008	0.753	0.2188	0.0020	2972	15	2910	13	2838	33	95.5
SMB17-234-82	2.29E+08	1251	405.6	3.08	28	16	57.1	9925	98.56	1	FALSE	1.963	0.023	0.169	0.002	0.569	0.0849	0.0006	1314	14	1103	8	1004	11	76.4
SMB17-234-83 <sup>d</sup>	2.10E+08	208.7	218	0.96	6	9	164.9	4198	99.07	1	FALSE	0.834	0.021	0.092	0.001	0.212	0.0660	0.0015	806	48	615	11	568	7	92.4
SMB17-234-84 <sup>d</sup>	2.06E+08	261	209	1.25	3	13	433.3	31933	99.03	1	FALSE	4.249	0.065	0.286	0.004	0.762	0.1078	0.0013	1763	22	1683	13	1620	21	91.9
SMB17-234-85 <sup>d</sup>	2.08E+08	276.8	198.8	1.39	1	11	1100.0	28610	99.38	1	FALSE	0.702	0.014	0.082	0.001	0.377	0.0621	0.0011	678	38	539	9	511	7	94.8
<b>SMB17-235 Run 1</b> Grid Zone 21T (WGS84) 289998 5099504																									
SMB17-235-7	2.32E+08	721	92.4	7.80	45	31	68.9	2111	97.75	1	FALSE	1.418	0.050	0.125	0.003	0.798	0.0830	0.0016	1269	38	896	21	757	16	59.6
SMB17-235-1	2.34E+08	595	83.4	7.13	-15	32	-213.3	106330	98.19	1	FALSE	1.995	0.072	0.166	0.003	0.604	0.0873	0.0021	1367	46	1113	25	992	19	72.6
SMB17-235-2 <sup>a</sup>	1.95E+08	468.3	10.98	42.65	7	10	152.3	7771	99.90	1	FALSE	0.864	0.025	0.104	0.002	0.384	0.0604	0.0011	618	39	632	14	636	9	100.7
SMB17-235-3 <sup>a</sup>	2.10E+08	149.4	101.8	1.47	18	18	100.0	781	99.68	1	FALSE	0.725	0.034	0.090	0.002	0.249	0.0592	0.0026	574	95	555	22	554	10	99.9
SMB17-235-4 <sup>a</sup>	1.85E+08	287.2	133	2.16	3	14	466.7	31200	99.70	1	FALSE	4.969	0.130	0.318	0.005	0.539	0.1132	0.0017	1851	27	1813	23	1780	25	96.1
SMB17-235-5 <sup>a</sup>	1.92E+08	138.6	117	1.18	-3	14	-466.7	13800	99.71	1	FALSE	0.762	0.031	0.093	0.002	0.217	0.0599	0.0020	600	72	574	19	571	9	99.4
SMB17-235-6 <sup>a</sup>	1.94E+08	223.3	312.1	0.72	5	13	260.0	17156	99.39	1	FALSE	6.674	0.180	0.372	0.007	0.744	0.1305	0.0017	2105	23	2068	23	2037	31	96.8



**Table A1.** Continued.

Corrections: 1 = threshold <sup>204</sup>Pb no correction (100 cps); 2 = threshold % <sup>204</sup>Pb-based correction (20% error) ; 3 = threshold % for <sup>208</sup>Pb-based correction (98.5 %Pb\*).

Sample	<sup>90</sup> Zr cps	U (ppm)	Th (ppm)	Th/U	<sup>204</sup> Pb cps	± 2σ	% ±	<sup>206</sup> Pb/ <sup>204</sup> Pb cps	%	Corrections			Isotopic ratios				Calculated ages								
										<sup>204</sup> Pb cps <sup>1</sup>	<sup>204</sup> Pb cps	<sup>204</sup> Pb cps	<sup>206</sup> Pb/ <sup>238</sup> U ± 2σ	<sup>206</sup> Pb/ <sup>235</sup> U ± 2σ	EC <sup>3</sup>	<sup>207</sup> Pb/ <sup>206</sup> Pb ± 2σ	<sup>207</sup> Pb/ <sup>235</sup> U ± 2σ	<sup>206</sup> Pb/ <sup>238</sup> U ± 2σ	<sup>207</sup> Pb/ <sup>235</sup> U ± 2σ	<sup>206</sup> Pb/ <sup>238</sup> U ± 2σ	<sup>206</sup> Pb/ <sup>235</sup> U ± 2σ	<sup>207</sup> Pb/ <sup>235</sup> U ± 2σ			
SMB17-235 - 8 <sup>a</sup>	2.04E+08	168.3	7.38	22.80	-2	13	-650.0	20680	99.58	1	FALSE	1.056	0.037	0.116	0.002	0.295	0.0660	0.0017	806	54	730	18	707	12	96.9
SMB17-235 - 9	2.15E+08	419.2	145	2.89	78	22	28.2	1098	98.22	1	FALSE	2.372	0.065	0.189	0.003	0.330	0.0916	0.0015	1459	31	1233	20	1114	16	76.4
SMB17-235 - 10 <sup>a</sup>	1.91E+08	111	87.9	1.26	22	12	54.5	479	99.57	1	FALSE	0.762	0.034	0.092	0.002	0.080	0.0604	0.0024	618	86	572	19	566	10	99.0
SMB17-235 - 11 <sup>a</sup>	1.90E+08	516	274.2	1.88	-2	13	-650.0	158800	99.93	1	FALSE	4.416	0.110	0.305	0.005	0.819	0.1054	0.0013	1721	23	1714	22	1713	25	99.5
SMB17-235 - 12 <sup>a</sup>	1.85E+08	355.3	198.9	1.79	9	12	133.3	3418	99.55	1	FALSE	0.728	0.024	0.086	0.001	0.173	0.0611	0.0016	643	56	555	14	534	8	96.3
SMB17-235 - 13	1.84E+08	245.3	64.3	3.81	7	13	185.7	4776	99.39	1	FALSE	1.336	0.042	0.136	0.002	0.325	0.0717	0.0016	977	45	862	19	820	12	83.9
SMB17-235 - 14 <sup>a</sup>	1.76E+08	144.1	21.54	6.69	16	14	87.5	1185	99.68	1	FALSE	1.163	0.045	0.130	0.003	0.170	0.0654	0.0023	787	74	784	23	787	14	100.0
SMB17-235 - 15 <sup>a</sup>	1.69E+08	164.3	94.6	1.74	19	15	78.9	679	98.92	1	FALSE	0.711	0.040	0.080	0.002	0.135	0.0647	0.0034	765	111	543	24	495	11	91.2
SMB17-235 - 16a	2.31E+08	865	73	11.85	42	30	71.4	2462	99.36	1	FALSE	1.033	0.037	0.111	0.002	0.521	0.0675	0.0017	853	52	720	18	680	13	94.5
SMB17-235 - 16a <sup>a</sup>	1.69E+08	204.7	113.2	1.81	14	15	107.1	3143	99.56	1	FALSE	2.558	0.078	0.217	0.004	0.541	0.0853	0.0018	1322	41	1287	22	1265	21	95.7
SMB17-235 - 17 <sup>ab</sup>	1.92E+08	193.9	122.1	1.59	-1	11	-1100.0	16950	99.67	1	FALSE	0.700	0.024	0.086	0.001	0.154	0.0592	0.0017	574	62	537	15	530	9	98.8
SMB17-235 - 18 <sup>a</sup>	1.81E+08	366.9	180.1	2.04	-5	13	-260.0	100120	99.79	1	FALSE	3.787	0.098	0.277	0.004	0.536	0.0990	0.0014	1606	26	1591	20	1575	22	98.1
SMB17-235 - 19	1.95E+08	225	131.8	1.71	20	13	65.0	969	98.09	1	FALSE	0.842	0.029	0.084	0.002	0.194	0.0728	0.0021	1008	59	620	17	521	9	84.0
SMB17-235 - 20a	2.20E+08	1171	8.93	131.13	27	17	63.0	4896	99.39	1	FALSE	0.997	0.028	0.108	0.002	0.197	0.0665	0.0013	822	41	702	14	664	10	94.6
SMB17-235 - 20a	1.51E+08	590	41.5	14.22	45	22	48.9	1789	98.37	1	FALSE	1.715	0.047	0.151	0.003	0.396	0.0823	0.0013	1252	31	1014	18	904	16	72.2
SMB17-235 - 21 <sup>a</sup>	1.89E+08	246	246.7	1.00	3	14	466.7	7743	99.71	1	FALSE	0.764	0.025	0.092	0.002	0.152	0.0597	0.0015	593	54	575	14	567	9	98.6
SMB17-235 - 22 <sup>ab</sup>	1.86E+08	227.5	226.4	1.00	-5	12	-240.0	19600	99.66	1	FALSE	0.709	0.023	0.086	0.001	0.005	0.0593	0.0016	578	59	543	14	533	9	98.2
SMB17-235 - 23 <sup>a</sup>	1.67E+08	208.6	89.8	2.32	22	14	63.6	2702	98.84	1	FALSE	4.647	0.130	0.297	0.005	0.334	0.1123	0.0022	1837	35	1756	24	1675	24	91.2
SMB17-235 - 24 <sup>a</sup>	1.89E+08	199.8	67.1	2.98	2	12	600.0	8970	99.76	1	FALSE	0.719	0.027	0.089	0.001	0.209	0.0581	0.0018	534	68	548	16	549	8	100.2
SMB17-235 - 25 <sup>a</sup>	1.93E+08	329	196	1.68	9	11	122.2	3100	99.71	1	FALSE	0.702	0.024	0.085	0.002	0.442	0.0592	0.0014	574	51	539	14	528	9	97.9
SMB17-235 - 26 <sup>a</sup>	1.89E+08	128.3	134	0.96	12	11	91.7	978	99.56	1	FALSE	0.764	0.029	0.090	0.002	0.400	0.0607	0.0019	629	67	576	17	558	9	96.9
SMB17-235 - 27	2.20E+08	131.9	23.56	5.60	-8	18	-225.0	21470	97.98	1	FALSE	1.867	0.085	0.156	0.004	0.437	0.0860	0.0032	1338	72	1067	31	935	19	69.9
SMB17-235 - 28 <sup>a</sup>	1.60E+08	707	251.8	2.81	216	45	20.8	790	97.36	-	2	3.350	0.310	0.252	0.006	0.741	0.0956	0.0035	1540	69	1495	69	1449	33	94.1
SMB17-235 - 29 <sup>a</sup>	1.75E+08	113.6	43.92	2.59	1	10	1000.0	34400	99.87	1	FALSE	4.946	0.140	0.322	0.005	0.365	0.1103	0.0020	1804	33	1808	24	1798	26	99.6
SMB17-235 - 30 <sup>a</sup>	1.73E+08	192.2	154.5	1.24	17	13	76.5	969	99.71	1	FALSE	0.722	0.029	0.089	0.002	0.521	0.0583	0.0019	541	71	550	17	548	9	99.5
SMB17-235 - 31 <sup>a</sup>	1.72E+05	213000	<LOD	na	4	12	300.0	5438	99.72	1	FALSE	0.967	0.032	0.112	0.002	0.307	0.0626	0.0015	695	51	685	16	684	11	99.9
SMB17-235 - 32 <sup>a</sup>	1.86E+08	141.1	57.39	2.46	5	11	220.0	7466	99.61	1	FALSE	3.605	0.100	0.268	0.004	0.386	0.0966	0.0017	1559	33	1548	23	1532	22	98.2
SMB17-235 - 33 <sup>ab</sup>	2.09E+08	79.75	41.79	1.91	2	15	750.0	3611	99.69	1	FALSE	0.705	0.044	0.086	0.002	0.309	0.0586	0.0033	552	123	537	26	531	10	98.9
SMB17-235 - 34 <sup>a</sup>	1.80E+08	220	86.3	2.55	6	14	233.3	9717	99.60	1	FALSE	3.459	0.097	0.262	0.004	0.378	0.0950	0.0017	1528	34	1518	23	1497	21	98.0
SMB17-235 - 35 <sup>a</sup>	1.93E+08	160.5	191.9	0.84	14	21	150.0	1071	99.70	1	FALSE	0.822	0.039	0.098	0.002	0.008	0.0602	0.0027	611	97	607	22	604	12	99.5
SMB17-235 - 36	2.31E+08	769	108	7.12	112	37	33.0	1028	96.28	-	2	1.608	0.120	0.139	0.003	0.500	0.0829	0.0041	1267	97	971	47	841	17	66.4
SMB17-235 - 37	2.02E+08	200	40.1	4.99	25	14	56.0	1140	99.86	1	FALSE	1.269	0.051	0.139	0.003	0.149	0.0658	0.0020	800	64	830	23	836	16	104.5
SMB17-235 - 38 <sup>a</sup>	1.77E+08	98.8	82.8	1.19	7	13	185.7	1214	99.69	1	FALSE	0.733	0.034	0.090	0.002	0.117	0.0586	0.0024	552	89	555	20	554	11	99.8
SMB17-235 - 39 <sup>ab</sup>	1.76E+08	81.1	59.22	1.37	1	12	1200.0	6853	99.50	1	FALSE	0.702	0.037	0.087	0.002	0.045	0.0587	0.0030	556	111	535	23	535	11	100.0
SMB17-235 - 40 <sup>a</sup>	1.78E+08	175.9	132.1	1.33	1	14	1400.0	14540	99.52	1	FALSE	0.725	0.030	0.085	0.001	0.317	0.0612	0.0021	646	74	552	18	527	8	95.4

**Table A1.** Continued.

Corrections: 1 = threshold <sup>204</sup>Pb no correction (100 cps); 2 = threshold % <sup>204</sup>Pb-based correction (20% error) ; 3 = threshold % for <sup>208</sup>Pb-based correction (98.5 %Pb\*).

Sample	<sup>90</sup> Zr cps	U (ppm)	Th (ppm)	Th/U	<sup>204</sup> Pb cps <sup>1</sup>	<sup>204</sup> Pb ± 2σ cps	% ± <sup>206</sup> Pb/ <sup>204</sup> Pb	cps	<sup>206</sup> Pb/ <sup>204</sup> Pb %	Corrections		Isotopic ratios				Calculated ages											
										± 2σ	%	<sup>207</sup> Pb/ <sup>235</sup> U ± 2σ	<sup>206</sup> Pb/ <sup>238</sup> U ± 2σ	<sup>207</sup> Pb/ <sup>206</sup> Pb ± 2σ	EC <sup>3</sup>	<sup>207</sup> Pb/ <sup>206</sup> Pb ± 2σ	<sup>207</sup> Pb/ ± 2σ	<sup>206</sup> Pb/ ± 2σ	<sup>207</sup> Pb/ ± 2σ	<sup>206</sup> Pb/ ± 2σ							
SMB17-235 - 41 <sup>a</sup>	1.89E+08	176.2	120.34	1.46	4	12	300.0	29125	100.00	1	FALSE	23.300	0.590	0.651	0.010	0.756	0.2583	0.0031	3236	19	3239	24	3232	39	99.9		
SMB17-235 - 42	2.26E+08	333.1	6.78	49.13	7	28	400.0	8986	98.12	1	FALSE	2.332	0.110	0.185	0.005	0.536	0.0913	0.0031	1453	65	1221	33	1094	25	75.3		
SMB17-235 - 42a <sup>a</sup>	1.80E+08	257.4	22	11.70	14	19	135.7	5439	98.91	1	FALSE	4.526	0.140	0.293	0.006	0.688	0.1113	0.0021	1821	34	1734	27	1657	31	91.0		
SMB17-235 - 43 <sup>a</sup>	1.77E+08	98.3	27.43	3.58	1	12	1200.0	21000	99.64	1	FALSE	2.435	0.082	0.213	0.004	0.296	0.0824	0.0021	1255	50	1250	24	1247	20	99.4		
SMB17-235 - 44	1.50E+08	136.3	170.9	0.80	321	45	14.0	44	58.00	-	3	1.020	1.100	0.089	0.008	0.933	0.0590	0.0770	567	2841	790	540	549	49	69.5		
SMB17-235 - 45 <sup>a</sup>	1.82E+08	169.9	103.33	1.64	-4	14	-350.0	59770	99.43	1	FALSE	5.831	0.160	0.345	0.005	0.497	0.1224	0.0020	1992	29	1950	24	1909	26	95.9		
SMB17-235 - 46	7.39E+07	113.2	72.4	1.56	26	15	57.7	169	95.30	1	FALSE	1.151	0.082	0.089	0.004	0.385	0.0957	0.0068	1542	134	780	43	549	21	70.4		
SMB17-235 - 47 <sup>a</sup>	1.89E+08	125.9	72.8	1.73	4	12	300.0	3118	99.64	1	FALSE	0.842	0.034	0.099	0.002	0.397	0.0618	0.0020	667	69	620	18	606	10	97.7		
SMB17-235 - 48 <sup>a</sup>	1.85E+08	87.46	41.54	2.11	5	12	240.0	6226	99.78	1	FALSE	6.023	0.170	0.358	0.006	0.466	0.1219	0.0022	1984	32	1977	25	1977	30	99.6		
SMB17-235 - 49 <sup>a,b</sup>	1.71E+08	89.2	76.9	1.16	6	12	200.0	1165	99.70	1	FALSE	0.707	0.037	0.086	0.002	0.174	0.0598	0.0029	596	105	538	22	534	11	99.2		
SMB17-235 - 50 <sup>a</sup>	1.99E+08	176.2	92.2	1.91	3	17	566.7	5260	99.20	1	FALSE	0.734	0.032	0.084	0.002	0.028	0.0639	0.0026	738	86	558	18	519	10	93.1		
SMB17-235 - 51	1.53E+08	122.1	48.5	2.52	16	17	106.3	604	98.51	1	FALSE	0.832	0.047	0.087	0.002	0.037	0.0700	0.0040	928	117	612	26	537	12	87.7		
<b>SMB17-235 Run 2 (in italics to distinguish from Run 1)</b>																											
SMB17-235 - 1 <sup>a</sup>	2.30E+08	326.8	235.1	1.39	28	14	50.0	1429	99.53	1	FALSE	0.745	0.016	0.088	0.001	0.220	0.0614	0.0012	653	42	565	9	546	7	96.6		
SMB17-235 - 2	2.19E+08	457.8	58.9	7.77	15	17	113.3	12593	98.65	1	FALSE	4.890	0.071	0.304	0.004	0.711	0.1169	0.0010	1909	15	1800	12	1710	20	89.6		
SMB17-235 - 3	2.49E+08	134.9	144.4	0.93	13	15	115.4	1248	97.82	1	FALSE	0.857	0.026	0.084	0.001	0.205	0.0752	0.0023	1074	61	627	14	520	8	82.9		
SMB17-235 - 4 <sup>a</sup>	2.01E+08	428.4	103.8	4.13	54	25	46.3	1133	99.45	1	FALSE	1.007	0.023	0.111	0.002	0.129	0.0656	0.0017	794	54	707	12	680	10	96.2		
SMB17-235 - 5 <sup>a</sup>	2.27E+08	136.6	61.3	2.23	30	16	53.3	3153	98.77	1	FALSE	12.880	0.190	0.497	0.007	0.361	0.1875	0.0022	2720	19	2670	14	2600	31	95.6		
SMB17-235 - 7 <sup>a</sup>	2.21E+08	264.4	118.5	2.23	4	18	450.0	7575	99.20	1	FALSE	0.719	0.021	0.083	0.001	0.069	0.0631	0.0019	712	64	549	13	512	8	93.2		
SMB17-235 - 9	2.04E+08	563.3	389	1.45	66	17	25.8	3258	94.46	1	FALSE	6.023	0.090	0.294	0.005	0.737	0.1481	0.0013	2324	15	1978	13	1661	22	71.5		
SMB17-235 - 10 <sup>a</sup>	2.17E+08	189.3	122.6	1.54	-1	12	-1200.0	24730	99.18	1	FALSE	0.893	0.025	0.099	0.001	0.253	0.0659	0.0018	803	57	649	14	606	8	93.3		
SMB17-235 - 12 <sup>a</sup>	1.95E+08	332.6	134.8	2.47	16	20	125.0	16500	96.30	1	FALSE	24.670	0.370	0.631	0.009	0.808	0.2820	0.0021	3374	12	3295	15	3152	36	93.4		
SMB17-235 - 13 <sup>a</sup>	2.24E+08	79	46.2	1.71	1	13	1300.0	9940	98.71	1	FALSE	0.885	0.038	0.094	0.002	0.206	0.0683	0.0028	878	85	640	20	576	9	90.0		
SMB17-235 - 14	1.94E+08	770	528	1.46	378	43	11.4	359	94.08	-	3	1.398	0.110	0.133	0.003	0.606	0.0741	0.0047	1044	128	878	47	807	15	77.3		
SMB17-235 - 15	2.44E+08	905	254	3.56	937	54	5.8	369	91.85	-	3	5.000	0.130	0.274	0.004	0.416	0.1320	0.0024	2125	32	1821	21	1559	19	73.4		
SMB17-235 - 16	2.12E+08	313.7	246.8	1.27	203	26	12.8	526	95.81	-	3	3.390	0.180	0.246	0.005	0.669	0.0985	0.0036	1596	68	1493	41	1416	28	88.7		
SMB17-235 - 17 <sup>a</sup>	2.16E+08	539	243	2.22	-1	12	-1200.0	184700	99.82	1	FALSE	3.302	0.037	0.256	0.003	0.549	0.0929	0.0007	1486	13	1481	9	1472	15	99.0		
SMB17-235 - 18 <sup>a</sup>	2.27E+08	349	375	0.93	26	13	50.0	5496	99.69	1	FALSE	4.707	0.059	0.311	0.004	0.560	0.1094	0.0009	1790	14	1768	11	1744	18	97.4		
SMB17-235 - 19	2.68E+08	1164	312.6	3.72	337	37	11.0	1060	95.46	-	3	3.094	0.092	0.211	0.004	0.766	0.1062	0.0016	1735	28	1430	23	1233	20	71.1		
SMB17-235 - 20 <sup>a</sup>	2.18E+08	445	12.33	36.09	19	13	68.4	3284	99.51	1	FALSE	0.944	0.016	0.106	0.001	0.140	0.0643	0.0010	752	32	674	9	647	7	95.9		
SMB17-235 - 21 <sup>a</sup>	2.24E+08	465	241.6	1.92	46	16	34.8	4787	98.80	1	FALSE	5.999	0.080	0.343	0.005	0.806	0.1262	0.0009	2046	12	1975	12	1899	22	92.8		
SMB17-235 - 22 <sup>a</sup>	2.43E+08	245.2	93.2	2.63	16	13	81.3	7713	99.60	1	FALSE	6.244	0.082	0.361	0.004	0.514	0.1254	0.0012	2034	17	2010	12	1986	21	97.6		
SMB17-235 - 23 <sup>a</sup>	2.24E+08	2099	501.1	4.19	121	27	22.3	6149	99.43	-	-	3.387	0.047	0.256	0.003	0.786	0.0951	0.0005	1531	10	1501	11	1468	17	95.9		
SMB17-235 - 25 <sup>a</sup>	2.31E+08	255.8	23.37	10.95	17	14	82.4	13476	98.67	1	FALSE	25.840	0.270	0.661	0.008	0.679	0.2821	0.0014	3375	8	3340	10	3272	30	97.0		
SMB17-235 - 26 <sup>a</sup>	2.25E+08	313.1	166.9	1.88	2	9	593.3	89933	99.86	1	FALSE	4.864	0.056	0.321	0.004	0.579	0.1097	0.0007	1794	12	1798	9	1794	18	100.0		

Table A1. Continued.

Corrections: 1 = threshold <sup>204</sup>Pb no correction (100 cps); 2 = threshold % <sup>204</sup>Pb-based correction (20% error) ; 3 = threshold % for <sup>208</sup>Pb-based correction (98.5 %Pb\*).

Sample	<sup>90</sup> Zr cps	U (ppm)	Th (ppm)	Th/U	<sup>204</sup> Pb cps <sup>1</sup>	<sup>204</sup> Pb cps ± 2σ	% ± <sup>206</sup> Pb/ <sup>204</sup> Pb	cps	Pb <sup>+2</sup> %	Corrections			Isotopic ratios				Calculated ages								
										± 2σ	<sup>206</sup> Pb/ <sup>238</sup> U ± 2σ	<sup>206</sup> Pb/ <sup>235</sup> U ± 2σ	EC <sup>3</sup>	<sup>207</sup> Pb/ <sup>206</sup> Pb ± 2σ	<sup>207</sup> Pb/ <sup>206</sup> Pb ± 2σ	<sup>207</sup> Pb/ <sup>235</sup> U ± 2σ	<sup>206</sup> Pb/ <sup>238</sup> U ± 2σ	<sup>207</sup> Pb/ <sup>206</sup> Pb ± 2σ	<sup>206</sup> Pb/ <sup>238</sup> U ± 2σ	<sup>207</sup> Pb/ <sup>235</sup> U ± 2σ	<sup>206</sup> Pb/ <sup>238</sup> U ± 2σ				
SMB17-235 - 27 <sup>a</sup>	2.24E+08	177.3	155.4	1.14	30	17	56.7	815	98.83	1	FALSE	0.963	0.032	0.101	0.002	0.275	0.0689	0.0022	896	66	683	17	619	9	90.7
SMB17-235 - 28 <sup>a</sup>	2.25E+08	112.3	91.1	1.23	4	11	275.0	20173	98.47	1	FALSE	14.480	0.200	0.521	0.007	0.756	0.2006	0.0016	2831	13	2780	13	2706	30	95.6
SMB17-235 - 29	2.15E+08	128	207.7	0.62	66	18	27.3	896	97.51	1	FALSE	6.600	0.100	0.346	0.005	0.540	0.1378	0.0018	2200	23	2058	14	1913	22	87.0
SMB17-235 - 32 <sup>a</sup>	2.24E+08	105.2	71.8	1.47	7	11	157.1	7914	99.70	1	FALSE	7.195	0.097	0.393	0.005	0.487	0.1329	0.0013	2137	17	2136	12	2139	23	100.1
SMB17-235 - 34 <sup>a</sup>	2.32E+08	951	158.1	6.02	524	40	7.6	327	94.69	-	3	1.092	0.073	0.123	0.002	0.534	0.0636	0.0032	728	107	745	36	748	12	100.3
SMB17-235 - 35	2.50E+08	566.1	120.6	4.69	174	26	14.9	1417	97.04	-	3	4.751	0.110	0.292	0.004	0.541	0.1177	0.0019	1922	29	1775	19	1653	20	86.0
SMB17-235 - 37 <sup>a</sup>	2.19E+08	128.8	62.4	2.06	1	11	1100.0	40700	99.73	1	FALSE	2.949	0.048	0.242	0.003	0.373	0.0885	0.0012	1393	26	1393	12	1396	16	100.2
SMB17-235 - 38 <sup>a</sup>	2.02E+08	163.2	105.9	1.54	31	17	54.8	3339	98.29	1	FALSE	12.840	0.220	0.491	0.007	0.659	0.1891	0.0021	2734	18	2667	16	2574	31	94.1
SMB17-235 - 39 <sup>a</sup>	2.53E+08	757	290	2.61	88	42	47.7	6318	98.99	1	FALSE	15.290	0.170	0.534	0.007	0.544	0.2083	0.0012	2892	9	2833	11	2759	28	95.4
SMB17-235 - 41	2.17E+08	973	159.5	6.10	173	31	17.9	1343	97.41	-	3	2.094	0.062	0.177	0.002	0.407	0.0855	0.0020	1327	45	1145	21	1053	13	79.3
SMB17-235 - 42 <sup>a</sup>	2.19E+08	125.3	33.37	3.75	14	10	71.4	4514	99.14	1	FALSE	7.024	0.100	0.378	0.005	0.597	0.1350	0.0014	2164	18	2113	13	2066	25	95.5
SMB17-235 - 43 <sup>a</sup>	2.26E+08	198.2	105.1	1.89	61	16	26.2	1625	98.61	1	FALSE	6.870	0.120	0.366	0.005	0.601	0.1367	0.0019	2186	24	2095	16	2010	22	92.0
SMB17-235 - 44	2.29E+08	490	154.9	3.16	395	40	10.1	353	92.91	-	3	2.660	0.140	0.194	0.003	0.642	0.0990	0.0037	1605	70	1309	40	1140	18	71.0
SMB17-235 - 45 <sup>a</sup>	2.46E+08	1049	81.5	12.87	105	23	21.9	1769	98.93	-	-	1.119	0.043	0.124	0.002	0.379	0.0654	0.0020	787	64	765	19	756	10	96.0
SMB17-235 - 46	2.01E+08	354.1	49.2	7.20	17	14	82.4	12271	96.19	1	FALSE	11.890	0.140	0.455	0.006	0.647	0.1896	0.0014	2739	12	2596	11	2417	26	88.3
SMB17-235 - 47 <sup>a</sup>	2.16E+08	276.3	115.1	2.40	384	39	10.2	320	94.67	-	3	5.170	0.250	0.319	0.006	0.692	0.1168	0.0043	1908	66	1838	42	1786	29	93.6
SMB17-235 - 48	2.35E+08	687	40.7	16.88	27	15	55.6	4344	98.56	1	FALSE	1.348	0.021	0.127	0.002	0.144	0.0770	0.0010	1121	26	866	9	773	9	68.9
SMB17-235 - 49 <sup>a</sup>	2.26E+08	181.4	121.2	1.50	23	14	60.9	4035	99.83	1	FALSE	6.381	0.093	0.370	0.005	0.613	0.1255	0.0012	2036	17	2029	13	2028	22	99.6
SMB17-235 - 50 <sup>a</sup>	2.61E+08	518	34.8	14.89	15	27	180.0	5200	99.20	1	FALSE	1.059	0.041	0.112	0.002	0.392	0.0693	0.0025	908	74	733	20	684	11	93.3
SMB17-235 - 51 <sup>a</sup>	2.10E+08	826	49.7	16.62	7	16	228.6	47314	99.50	1	FALSE	4.611	0.059	0.304	0.004	0.687	0.1100	0.0009	1800	15	1751	11	1711	20	95.1
SMB17-235 - 54	1.98E+08	698	317	2.20	159	24	15.1	1928	94.21	-	3	7.466	0.120	0.341	0.005	0.698	0.1587	0.0015	2442	16	2168	15	1889	22	77.4
SMB17-235 - 55	1.72E+08	258.6	227.3	1.14	175	28	16.0	441	93.44	-	3	4.280	0.220	0.259	0.005	0.685	0.1188	0.0045	1938	68	1680	43	1482	26	76.5
SMB17-235 - 56	2.12E+08	312.3	230	1.36	192	23	12.0	623	96.37	-	3	4.010	0.160	0.274	0.004	0.438	0.1062	0.0035	1735	60	1630	34	1558	19	89.8
SMB17-235 - 57	2.18E+08	356	57.4	6.20	156	22	14.1	1011	95.89	-	3	5.720	0.130	0.316	0.005	0.546	0.1311	0.0022	2113	29	1932	20	1768	23	83.7
SMB17-235 - 58	2.11E+08	475.3	67.2	7.07	73	18	24.7	1056	97.77	1	FALSE	1.334	0.024	0.119	0.001	0.241	0.0812	0.0012	1226	29	860	11	726	8	84.5
SMB17-235 - 59	2.19E+08	40	53.3	0.75	14	17	121.4	1557	94.83	1	FALSE	10.980	0.500	0.420	0.017	0.945	0.1894	0.0028	2737	24	2508	49	2256	81	82.4
SMB17-235 - 60 <sup>a</sup>	1.93E+08	228.3	73.8	3.09	-5	14	-280.0	85600	99.72	1	FALSE	4.273	0.100	0.297	0.006	0.710	0.1038	0.0015	1693	27	1686	20	1682	29	99.3
SMB17-235 - 62 <sup>a</sup>	2.13E+08	543	121.2	4.48	118	21	17.8	747	97.53	-	3	1.007	0.064	0.115	0.002	0.456	0.0628	0.0035	701	119	701	33	702	10	100.2
SMB17-235 - 63 <sup>a</sup>	2.14E+08	132	75.4	1.75	13	10	76.9	2623	99.30	1	FALSE	2.243	0.042	0.197	0.003	0.308	0.0825	0.0014	1257	33	1193	13	1159	16	92.2
SMB17-235 - 64 <sup>a</sup>	2.05E+08	561	14.8	37.91	42	18	42.9	6026	99.01	1	FALSE	5.990	0.081	0.344	0.005	0.788	0.1257	0.0009	2039	12	1974	12	1905	23	93.4
SMB17-235 - 65	1.91E+08	419	260	1.61	55	18	32.7	955	98.23	1	FALSE	1.049	0.019	0.102	0.002	0.181	0.0743	0.0016	1050	43	728	10	627	9	86.1
SMB17-235 - 67	2.07E+08	55.69	37.86	1.47	19	15	78.9	1240	98.05	1	FALSE	5.620	0.160	0.325	0.006	0.667	0.1258	0.0025	2040	35	1913	25	1812	30	88.8
SMB17-235 - 68 <sup>a</sup>	1.86E+08	1085	242.9	4.47	307	41	13.4	536	96.07	-	3	1.119	0.079	0.118	0.002	0.479	0.0678	0.0040	862	122	759	38	721	11	95.0
SMB17-235 - 69 <sup>a</sup>	2.16E+08	653.9	87.76	7.45	11	11	100.0	20255	99.66	1	FALSE	3.300	0.037	0.253	0.003	0.562	0.0943	0.0006	1513	13	1482	8	1452	15	96.0
SMB17-235 - 70 <sup>a</sup>	2.02E+08	327.6	174.1	1.88	74	18	24.3	1682	98.75	1	FALSE	4.887	0.064	0.305	0.004	0.456	0.1157	0.0010	1891	15	1799	11	1716	18	90.7
SMB17-235 - 71	2.45E+08	513	9.68	53	174	39	22.4	1484	92.85	-	2	9.300	0.220	0.374	0.007	0.884	0.1805	0.0018	2657	17	2366	22	2046	31	77.0

**Table A1.** Continued.

Corrections: 1 = threshold <sup>204</sup>Pb no correction (100 cps); 2 = threshold % <sup>204</sup>Pb-based correction (20% error) ; 3 = threshold % for <sup>208</sup>Pb-based correction (98.5 %Pb\*).

Sample	<sup>90</sup> Zr cps	U (ppm)	Th (ppm)	Th/U	<sup>204</sup> Pb cps <sup>1</sup>	<sup>204</sup> Pb cps ± 2σ	% ± <sup>204</sup> Pb cps	<sup>206</sup> Pb cps	<sup>206</sup> Pb/ <sup>204</sup> Pb %	Corrections	Isotopic ratios			Calculated ages											
											<sup>207</sup> Pb/ <sup>235</sup> U ± 2σ	<sup>206</sup> Pb/ <sup>238</sup> U ± 2σ	<sup>207</sup> Pb/ <sup>206</sup> Pb ± 2σ	<sup>207</sup> Pb/ <sup>206</sup> Pb ± 2σ	<sup>206</sup> Pb/ <sup>235</sup> U ± 2σ	<sup>207</sup> Pb/ <sup>235</sup> U ± 2σ	<sup>206</sup> Pb/ <sup>238</sup> U ± 2σ								
SMB17-235 - 72 <sup>a</sup>	1.98E+08	255.3	109.3	2.34	-5	11	-220.0	27690	99.30	1	FALSE	0.746	0.020	0.086	0.001	0.067	0.0624	0.0017	688	58	564	12	533	7	94.5
SMB17-235 - 73 <sup>a</sup>	2.26E+08	38.6	19.34	2.00	-5	10	-208.7	20420	98.81	1	FALSE	7.520	0.170	0.392	0.007	0.489	0.1390	0.0024	2215	30	2171	21	2133	33	96.3
SMB17-235 - 74 <sup>a</sup>	2.32E+08	456	95.7	4.76	8	10	125.0	38563	99.42	1	FALSE	12.681	0.130	0.499	0.006	0.668	0.1842	0.0009	2691	8	2656	10	2608	25	96.9
SMB17-235 - 76 <sup>a</sup>	2.19E+08	183.6	95.7	1.92	-6	14	-233.3	20310	99.24	1	FALSE	0.690	0.020	0.081	0.001	0.139	0.0617	0.0017	664	59	532	12	502	7	94.3
SMB17-235 - 77	2.35E+08	455.5	119.5	3.81	160	29	18.1	1138	96.97	-	3	4.530	0.130	0.286	0.004	0.481	0.1143	0.0025	1869	39	1738	22	1623	21	86.8
SMB17-235 - 78	2.50E+08	1195	110.6	10.80	229	36	15.7	1937	92.13	-	3	5.600	0.120	0.265	0.004	0.841	0.1533	0.0017	2383	19	1915	19	1513	19	63.5
SMB17-235 - 79 <sup>a</sup>	2.36E+08	946	13.9	68.06	21	16	76.2	6800	99.50	1	FALSE	0.971	0.013	0.107	0.001	0.858	0.0654	0.0007	786	21	689	7	658	7	95.5
SMB17-235 - 80	2.41E+08	426	83.2	5.12	60	19	31.7	2038	97.38	1	FALSE	3.053	0.061	0.214	0.004	0.823	0.1036	0.0011	1690	20	1420	15	1247	22	73.8
SMB17-235 - 81 <sup>a</sup>	2.02E+08	168.1	121.9	1.38	10	12	120.0	6970	98.91	1	FALSE	5.358	0.088	0.323	0.004	0.486	0.1197	0.0015	1952	22	1877	14	1802	20	92.3
SMB17-235 - 82 <sup>a</sup>	2.11E+08	90.7	62.95	1.44	28	13	46.4	1450	98.91	1	FALSE	5.838	0.100	0.340	0.005	0.558	0.1239	0.0016	2013	23	1950	15	1886	24	93.7
SMB17-235 - 83	2.40E+08	426	189	2.25	374	43	11.5	452	93.67	-	3	4.990	0.200	0.286	0.006	0.688	0.1260	0.0031	2043	43	1813	34	1621	28	79.3
SMB17-235 - 84	1.90E+08	586.2	465	1.26	462	48	10.4	435	93.93	-	3	4.200	0.150	0.263	0.005	0.598	0.1146	0.0031	1874	49	1671	30	1505	23	80.3
SMB17-235 - 85 <sup>a</sup>	2.27E+08	432.8	39.41	10.98	-9	13	-144.4	203100	99.69	1	FALSE	5.781	0.069	0.346	0.004	0.548	0.1207	0.0009	1967	13	1943	10	1914	19	97.3
SMB17-235 - 86	2.20E+08	312.7	264.9	1.18	104	22	21.2	1886	96.08	-	2	11.540	0.200	0.454	0.006	0.475	0.1832	0.0022	2682	20	2567	16	2412	28	89.9
SMB17-235 - 87 <sup>a</sup>	2.09E+08	535.4	13.56	39.48	15	17	113.3	4911	99.22	1	FALSE	0.923	0.019	0.101	0.001	0.792	0.0658	0.0012	800	38	663	10	619	7	93.3

**NOTES:** <sup>a</sup>grains between 90 and 102% concordant; <sup>b</sup>grains used in weighted mean calculations for youngest clusters; <sup>1</sup>after Hg correction; <sup>2</sup>radiogenic Pb; <sup>3</sup>error correction. Abbreviations: cps = counts per second.



**Table A2.** LA-ICP-MS U-Pb isotopic analyses of zircon reference materials analyzed at the University of New Brunswick.

Corrections: 1 = threshold <sup>204</sup>Pb no correction (100 cps); 2 = threshold % <sup>204</sup>Pb-based correction(20% error) ; 3 = threshold % for <sup>208</sup>Pb-based correction (98.5 %Pb\*).

Sample	<sup>90</sup> Zr cps	U (ppm)	Th (ppm)	Th/U	<sup>204</sup> Pb cps <sup>1</sup>	<sup>204</sup> Pb ± 2σ	% ±	<sup>206</sup> Pb/ <sup>204</sup> Pb	Pb cps	% Pb* <sup>2</sup>	Corrections	Isotopic ratios			Calculated ages										
												<sup>207</sup> Pb/ <sup>235</sup> U ± 2σ	<sup>206</sup> Pb/ <sup>238</sup> U ± 2σ	EC <sup>3</sup>	<sup>207</sup> Pb/ <sup>206</sup> Pb ± 2σ	<sup>207</sup> Pb/ ± 2σ	<sup>206</sup> Pb/ ± 2σ	<sup>207</sup> Pb/ ± 2σ	<sup>206</sup> Pb/ ± 2σ	% conc					
<b>Run 1 for both samples</b>																									
FC-1 - 1	1.85E+08	317.2	191.6	1.66	12	12	100.0	4988	99.91	1	FALSE	1.950	0.053	0.186	0.003	0.301	0.0759	0.0013	1092	34	1097	18	1101	15	100.8
FC-1 - 2	1.83E+08	260.3	164	1.59	7	13	185.7	6950	99.79	1	FALSE	1.955	0.055	0.186	0.003	0.343	0.0765	0.0014	1108	37	1099	19	1097	16	99.0
FC-1 - 3	1.84E+08	307.3	183.6	1.67	14	12	85.7	4061	99.93	1	FALSE	1.961	0.054	0.186	0.003	0.302	0.0763	0.0013	1103	34	1101	18	1102	15	99.9
FC-1 - 4	1.84E+08	336.7	159.83	2.11	13	13	100.0	4722	99.86	1	FALSE	1.933	0.051	0.185	0.003	0.105	0.0758	0.0013	1090	34	1092	18	1093	15	100.2
FC-1 - 5	1.81E+08	408.4	260.8	1.57	-2	11	-550.0	73640	99.94	1	FALSE	1.969	0.052	0.187	0.003	0.305	0.0767	0.0012	1113	31	1104	18	1103	15	99.1
FC-1 - 6	1.82E+08	178	77.75	2.29	4	12	300.0	8040	99.83	1	FALSE	1.957	0.058	0.187	0.003	0.284	0.0758	0.0015	1090	40	1099	20	1102	16	101.1
FC-1 - 7	1.81E+08	157.4	62.75	2.51	-1	12	-1200.0	27770	99.82	1	FALSE	1.930	0.058	0.185	0.003	0.284	0.0753	0.0016	1077	43	1089	20	1092	16	101.4
FC-1 - 8	1.80E+08	284.9	169.9	1.68	3	12	400.0	16860	99.91	1	FALSE	1.941	0.052	0.185	0.003	0.246	0.0753	0.0012	1075	32	1096	19	1096	15	101.9
FC-1 - 9	1.79E+08	201.3	111.56	1.80	-3	10	-333.3	35900	99.82	1	FALSE	1.974	0.057	0.186	0.003	0.439	0.0772	0.0014	1126	36	1105	20	1102	16	97.8
FC-1 - 10	1.93E+08	128.8	53.3	2.42	4	13	325.0	5843	99.73	1	FALSE	1.933	0.068	0.184	0.003	0.057	0.0770	0.0024	1121	62	1090	24	1090	18	97.2
FC-1 - 11	1.70E+08	473.6	294.2	1.61	-4	11	-275.0	82400	99.92	1	FALSE	1.960	0.051	0.187	0.003	0.290	0.0767	0.0012	1112	31	1101	18	1106	15	99.4
FC-1 - 12	1.71E+08	473.7	292.6	1.62	-2	13	-650.0	82600	99.94	1	FALSE	1.948	0.052	0.186	0.003	0.312	0.0759	0.0012	1091	32	1097	18	1102	15	101.0
FC-1 - 14	1.70E+08	101.69	38.29	2.66	1	12	1200.0	17300	99.84	1	FALSE	1.936	0.066	0.185	0.003	0.221	0.0754	0.0020	1079	53	1090	23	1095	17	101.5
FC-1 - 15	1.70E+08	273.1	151.4	1.80	7	11	157.1	6613	99.88	1	FALSE	1.958	0.053	0.185	0.003	0.331	0.0765	0.0013	1108	34	1101	19	1094	15	98.7
FC-1 - 16	1.64E+08	288.7	164.1	1.76	-3	13	-433.3	49110	99.99	1	FALSE	1.953	0.057	0.187	0.003	0.248	0.0753	0.0015	1077	40	1100	19	1105	16	102.7
FC-1 - 17	1.75E+08	181.5	77.98	2.33	9	12	133.3	3429	99.85	1	FALSE	1.925	0.059	0.184	0.003	0.265	0.0757	0.0016	1087	42	1088	20	1088	16	100.1
FC-1 - 18	1.67E+08	321.5	187.6	1.71	16	13	81.3	3376	99.88	1	FALSE	1.965	0.052	0.186	0.003	0.134	0.0767	0.0013	1113	34	1103	18	1102	15	98.9
FC-1 - 19	1.65E+08	283	128.8	2.20	-2	11	-550.0	47040	99.92	1	FALSE	1.946	0.055	0.186	0.003	0.378	0.0760	0.0014	1095	37	1095	19	1101	15	100.5
Plesovice - 1	1.87E+08	702.1	65.47	10.72	6	12	200.0	6380	99.86	1	FALSE	0.394	0.012	0.053	0.001	0.218	0.0538	0.0012	363	50	337	9	333	5	98.7
Plesovice - 2	1.87E+08	406.1	32.58	12.46	16	11	68.8	1358	99.87	1	FALSE	0.380	0.013	0.052	0.001	0.486	0.0527	0.0014	316	60	326	10	328	5	100.6
Plesovice - 3	1.84E+08	466.2	40.14	11.61	4	14	350.0	6035	99.76	1	FALSE	0.381	0.013	0.052	0.001	0.111	0.0537	0.0014	358	59	328	10	325	5	98.9
Plesovice - 4	1.86E+08	395.7	35.1	11.27	1	11	1100.0	20550	99.83	1	FALSE	0.379	0.013	0.052	0.001	0.041	0.0529	0.0015	325	64	325	10	326	5	100.2
Plesovice - 5	1.86E+08	664.6	60.13	11.05	8	12	150.0	4385	99.77	1	FALSE	0.398	0.012	0.053	0.001	0.266	0.0542	0.0012	379	50	340	9	335	5	98.5
Plesovice - 6	1.81E+08	813	69.8	11.65	3	12	400.0	13747	99.84	1	FALSE	0.389	0.011	0.053	0.001	0.286	0.0529	0.0010	322	43	333	8	334	5	100.2
Plesovice - 7	1.83E+08	547.8	47.84	11.45	-9	11	-122.2	28220	99.83	1	FALSE	0.396	0.012	0.053	0.001	0.286	0.0533	0.0011	342	47	338	9	334	5	98.6
Plesovice - 8	1.81E+08	685.6	74.99	9.14	11	11	100.0	3171	99.76	1	FALSE	0.392	0.012	0.053	0.001	0.043	0.0537	0.0012	358	50	335	9	330	5	98.4
Plesovice - 9	1.80E+08	629.2	56.86	11.07	1	12	1200.0	32270	99.80	1	FALSE	0.392	0.012	0.053	0.001	0.011	0.0540	0.0013	371	54	336	9	333	5	99.1
Plesovice - 10	1.79E+08	538.7	47.07	11.44	-3	10	-366.7	27390	99.81	1	FALSE	0.384	0.013	0.052	0.001	0.193	0.0536	0.0014	354	59	329	10	329	5	100.1
Plesovice - 11	1.79E+08	640.3	58.45	10.95	9	11	122.2	3600	99.87	1	FALSE	0.383	0.012	0.052	0.001	0.057	0.0536	0.0013	354	55	329	9	329	5	100.0
Plesovice - 12	1.75E+08	598.8	53.39	11.22	-21	11	-52.4	29650	99.79	1	FALSE	0.385	0.011	0.052	0.001	0.294	0.0541	0.0011	373	46	330	8	326	5	98.8
Plesovice - 13	1.77E+08	829.5	84.84	9.78	-3	11	-366.7	41960	99.84	1	FALSE	0.388	0.011	0.053	0.001	0.113	0.0533	0.0011	339	47	332	8	331	5	99.4
Plesovice - 14	1.84E+08	678.9	62.81	10.81	1	13	1300.0	34640	99.80	1	FALSE	0.394	0.013	0.053	0.001	0.122	0.0535	0.0013	350	55	337	9	333	5	99.0
Plesovice - 15	1.70E+08	563.9	49.19	11.46	10	12	120.0	2781	99.89	1	FALSE	0.388	0.012	0.054	0.001	0.184	0.0522	0.0012	294	52	332	9	336	5	101.2
Plesovice - 16	1.77E+08	863.1	114.8	7.52	-1	13	-1300.0	43570	99.84	1	FALSE	0.396	0.011	0.053	0.001	0.162	0.0536	0.0010	352	42	339	8	335	5	98.8
Plesovice - 17	1.88E+08	846.2	90.5	9.35	2	14	700.0	21775	99.93	1	FALSE	0.387	0.013	0.053	0.001	0.287	0.0523	0.0013	299	57	332	9	335	5	101.1
Plesovice - 18	1.89E+08	962.4	109.37	8.80	6	15	250.0	8222	99.90	1	FALSE	0.394	0.012	0.054	0.001	0.289	0.0536	0.0012	354	51	337	9	336	5	99.6
Plesovice - 19	1.83E+08	725.5	69.89	10.38	11	15	136.4	3352	100.00	1	FALSE	0.384	0.012	0.053	0.001	0.287	0.0525	0.0013	307	56	329	9	334	5	101.5

Table A2. Continued.

Corrections: 1 = threshold <sup>204</sup>Pb no correction (100 cps); 2 = threshold % <sup>204</sup>Pb-based correction(20% error) ; 3 = threshold % for <sup>208</sup>Pb-based correction (98.5 %Pb\*).

Sample	<sup>90</sup> Zr cps	U (ppm)	Th (ppm)	Th/U	<sup>204</sup> Pb cps <sup>1</sup>	<sup>204</sup> Pb ± 2σ	% ± 2σ	<sup>206</sup> Pb/ <sup>204</sup> Pb	Pb cps	Pb <sup>2</sup>	Pb <sup>2</sup>	Pb <sup>2</sup>	Corrections			Isotopic ratios			Calculated ages						
													1	2	3	<sup>206</sup> Pb/ <sup>238</sup> U ± 2σ	<sup>207</sup> Pb/ <sup>206</sup> Pb ± 2σ	EC <sup>3</sup>	<sup>207</sup> Pb/ <sup>206</sup> Pb ± 2σ	<sup>207</sup> Pb/ ± 2σ	<sup>207</sup> Pb/ ± 2σ	<sup>206</sup> Pb/ ± 2σ	<sup>238</sup> U	% conc	
<b>Run 2 for both samples</b>																									
FC-1 - 1	2.34E+08	236.3	86.18	2.74	15	13	86.7	3925	99.79	1	FALSE	1.959	0.031	0.186	0.002	0.438	0.0768	0.0009	1111	24	1100	11	1101	12	100.0
FC-1 - 2	2.19E+08	289.9	174.8	1.66	8	12	150.0	8615	99.77	1	FALSE	1.947	0.031	0.186	0.002	0.353	0.0760	0.0010	1088	26	1096	11	1098	12	100.0
FC-1 - 3	2.14E+08	167.8	76.28	2.20	2	11	550.0	19850	99.70	1	FALSE	1.947	0.036	0.186	0.002	0.174	0.0756	0.0013	1075	34	1096	12	1100	12	100.0
FC-1 - 4	2.09E+08	118.82	39.87	2.98	-4	12	-300.0	27460	99.71	1	FALSE	1.945	0.038	0.185	0.002	0.100	0.0757	0.0015	1080	38	1095	13	1096	13	100.0
FC-1 - 5	2.12E+08	238.9	111.62	2.14	-1	11	-1100.0	55880	99.80	1	FALSE	1.948	0.029	0.186	0.002	0.119	0.0763	0.0010	1098	25	1097	10	1097	12	100.0
FC-1 - 6	2.08E+08	373.1	225	1.66	2	9	460.0	43165	99.82	1	FALSE	1.962	0.026	0.186	0.002	0.436	0.0767	0.0007	1115	19	1102	9	1099	12	98.2
FC-1 - 7	2.06E+08	405.1	265.3	1.53	10	10	100.0	9325	99.87	1	FALSE	1.949	0.025	0.187	0.002	0.253	0.0757	0.0008	1083	20	1098	9	1103	11	100.0
FC-1 - 8	2.09E+08	270.1	147.6	1.83	16	12	75.0	3926	99.79	1	FALSE	1.951	0.029	0.186	0.002	0.203	0.0762	0.0009	1094	25	1099	10	1098	12	99.3
FC-1 - 9	2.06E+08	252.2	136.4	1.85	-1	10	-1000.0	58040	99.75	1	FALSE	1.954	0.030	0.186	0.002	0.123	0.0760	0.0010	1095	24	1099	10	1097	12	99.3
FC-1 - 10	2.04E+08	181.6	73.3	2.48	12	9	78.3	3448	99.72	1	FALSE	1.945	0.036	0.186	0.002	0.244	0.0756	0.0012	1074	34	1095	12	1099	13	100.0
FC-1 - 12	2.01E+08	160.7	72	2.23	-7	9	-132.4	35790	99.69	1	FALSE	1.956	0.034	0.186	0.002	0.362	0.0763	0.0012	1100	30	1102	12	1097	12	99.9
FC-1 - 13	2.02E+08	324.3	193.2	1.68	8	11	137.5	9155	99.81	1	FALSE	1.952	0.027	0.187	0.002	0.288	0.0755	0.0009	1076	24	1098	9	1102	12	100.0
FC-1 - 14	2.02E+08	248.4	154.21	1.61	14	13	92.9	3977	99.71	1	FALSE	1.944	0.032	0.185	0.002	0.107	0.0762	0.0011	1092	30	1095	11	1094	12	99.3
FC-1 - 15	1.99E+08	123.71	51.7	2.39	7	11	157.1	3923	99.67	1	FALSE	1.963	0.036	0.187	0.002	0.205	0.0765	0.0013	1100	33	1101	12	1102	13	100.0
FC-1 - 17	1.99E+08	339.7	213.1	1.59	-2	10	-500.0	75500	99.82	1	FALSE	1.958	0.028	0.186	0.002	0.384	0.0764	0.0009	1101	22	1100	10	1102	12	100.0
FC-1 - 18	2.02E+08	162.8	90.1	1.81	9	11	122.2	4013	99.69	1	FALSE	1.927	0.033	0.184	0.002	0.103	0.0762	0.0012	1095	31	1089	12	1091	12	100.0
FC-1 - 19	2.01E+08	255.6	153.8	1.66	-10	10	-100.0	57110	99.76	1	FALSE	1.963	0.031	0.187	0.002	0.209	0.0765	0.0011	1101	27	1102	11	1103	12	100.0
FC-1 - 20	2.23E+08	112.8	43.68	2.58	-3	14	-466.7	26030	99.67	1	FALSE	1.953	0.053	0.186	0.003	0.149	0.0763	0.0019	1102	53	1098	18	1098	14	99.6
Plesovice1 - 1	2.19E+08	694.4	64.95	10.69	7	13	185.7	6663	99.91	1	FALSE	0.387	0.007	0.054	0.001	0.175	0.0529	0.0009	315	39	332	5	336	4	101.4
Plesovice1 - 2	2.03E+08	702.5	65.23	10.77	-7	11	-157.1	45880	99.84	1	FALSE	0.394	0.007	0.054	0.001	0.211	0.0524	0.0008	297	35	337	5	340	4	101.0
Plesovice1 - 3	2.01E+08	480.4	38.94	12.34	9	11	122.2	3452	99.87	1	FALSE	0.396	0.009	0.054	0.001	0.330	0.0531	0.0010	321	43	338	6	340	4	100.6
Plesovice1 - 4	2.01E+08	751.2	75.86	9.90	-8	10	-125.0	48580	99.69	1	FALSE	0.403	0.007	0.054	0.001	0.595	0.0545	0.0008	384	33	343	5	336	4	98.0
Plesovice1 - 5	1.97E+08	495.1	42.89	11.54	1	11	1100.0	31750	99.72	1	FALSE	0.405	0.008	0.054	0.001	0.207	0.0540	0.0010	364	43	345	6	341	4	98.7
Plesovice1 - 6	1.95E+08	767.3	75.02	10.23	-3	12	-400.0	48120	99.79	1	FALSE	0.398	0.007	0.054	0.001	0.221	0.0532	0.0009	329	37	340	5	339	4	99.7
Plesovice1 - 7	1.94E+08	811.4	65.93	12.31	1	10	1000.0	50840	99.81	1	FALSE	0.396	0.007	0.054	0.001	0.274	0.0531	0.0008	323	35	339	5	338	4	99.9
Plesovice1 - 8	1.92E+08	776.4	78.12	9.94	1	11	1100.0	47770	99.80	1	FALSE	0.393	0.008	0.054	0.001	0.225	0.0534	0.0010	330	43	336	6	337	4	100.3
Plesovice1 - 9	1.91E+08	1254.1	114.67	10.94	-13	10	-76.9	76540	99.80	1	FALSE	0.397	0.006	0.053	0.001	0.408	0.0542	0.0007	371	28	340	5	335	4	98.7
Plesovice1 - 10	1.93E+08	527	47.1	11.19	4	11	275.0	8243	99.64	1	FALSE	0.409	0.010	0.054	0.001	0.069	0.0549	0.0012	398	51	349	7	341	4	97.7
Plesovice2 - 1	2.25E+08	773.7	64.58	11.98	6	13	216.7	9037	99.90	1	FALSE	0.394	0.007	0.054	0.001	0.045	0.0529	0.0009	313	38	337	5	341	4	101.3
Plesovice2 - 2	2.13E+08	932.8	103.59	9.00	4	10	250.0	15828	99.88	1	FALSE	0.398	0.006	0.055	0.001	0.077	0.0529	0.0007	318	30	340	5	342	4	100.6
Plesovice2 - 3	2.04E+08	602.9	52.83	11.41	6	12	200.0	6623	99.82	1	FALSE	0.398	0.009	0.055	0.001	0.027	0.0529	0.0011	310	46	340	6	342	4	100.7
Plesovice2 - 4	2.02E+08	730.5	67.7	10.79	-1	10	-1000.0	48000	99.83	1	FALSE	0.400	0.008	0.055	0.001	0.256	0.0534	0.0009	337	38	341	6	342	4	100.3
Plesovice2 - 5	2.04E+08	394.1	30.72	12.83	2	11	550.0	12805	99.75	1	FALSE	0.392	0.008	0.053	0.001	0.025	0.0536	0.0011	339	45	336	6	333	4	99.1
Plesovice2 - 6	2.00E+08	643.1	58.64	10.97	12	13	108.3	3482	99.72	1	FALSE	0.403	0.008	0.054	0.001	0.168	0.0538	0.0010	347	43	343	6	339	4	98.9
Plesovice2 - 7	1.96E+08	899.1	94.83	9.48	-6	11	-183.3	56260	99.76	1	FALSE	0.397	0.007	0.053	0.001	0.336	0.0537	0.0008	348	33	339	5	335	4	98.8
Plesovice2 - 8	1.93E+08	446.3	36.21	12.33	5	9	200.0	5851	99.87	1	FALSE	0.390	0.009	0.053	0.001	0.171	0.0529	0.0010	317	44	334	6	335	4	100.2
Plesovice2 - 9	1.97E+08	677.9	71.72	9.45	3	10	333.3	14340	99.80	1	FALSE	0.395	0.008	0.054	0.001	0.245	0.0538	0.0009	352	38	338	6	336	4	99.5

NOTES: <sup>1</sup> after Hg correction; <sup>2</sup> radiogenic Pb; <sup>3</sup> error correction. Abbreviations: cps = counts per second.

## APPENDIX B

Location and sample information, organic-walled microfossils and trace fossils. Sample coordinates are in Grid Zone 21T (WGS84). Locations are indicated also on Figure 2 and shown in a stratigraphic column (Fig. B1).

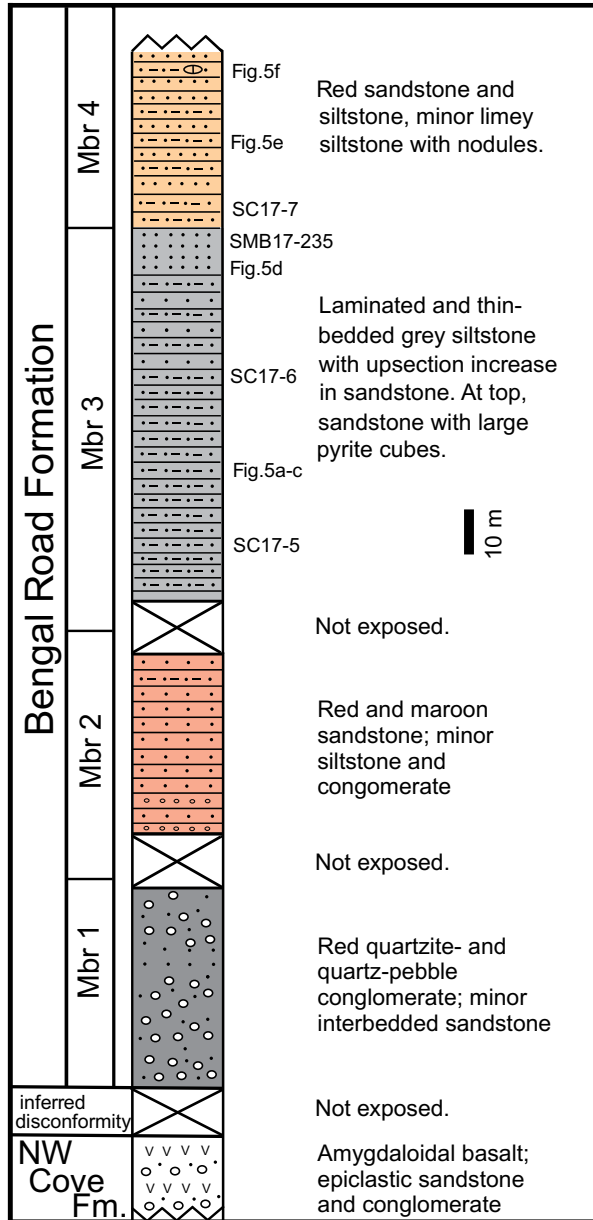


**Figure B1.** Stratigraphic interpretation of the southern limb of the southernmost syncline on the eastern shore of Scatarie Island (Fig. 2). Members 3 and 4 were logged in August 2017. Members 1 and 2 are schematic and based on notes made in 1991 when they were partially exposed. Abbreviation: NW Cove Fm = Northwest Cove Formation.

### Scatarie Island, Bengal Road Fm. Coastal section of upper part of Bengal Road Formation

SC17-5. 0289970, 5099472. Abundant dispersed organic matter and very scarce organic-walled microfossils that are limited to fragments without recognizable forms, except for a small filament of possible cyanobacteria (Fig. 6a).

SC17-6. 0289994, 5099484. Small amount of dispersed organic matter and very scarce organic-walled microfossils without recognizable forms, except for an acritarch assigned to *Polygonium* sp. (Fig. 6b).

SC17-7. 0289995, 5099517. Small amount of dispersed organic matter. Possible black carbonaceous fragments without recognizable forms.

### Hay Island, MacCodrum? Formation

1. Section on southern Hay Island at 0291878, 5099931. *Teichichnid* trace fossils (Fig. 7). Sample SC17-2, with small amount of dispersed organic matter, possible black carbonaceous fragments without recognizable morphologies. From same area at 0291885, 5099911, sample SC17-3, with small amount of dispersed organic matter, possible black carbonaceous fragments without recognizable morphologies. Among the maceration-resistant minerals are some idiomorphic zircon crystals. Also sample SC17-4, with no dispersed organic matter. Possible black carbonaceous fragments without recognizable shapes.

2. Section on northeastern Hay Island at 0292071, 5100170, cleaved dark grey siltstone with carbonate nodules. Sample SC17-8, with small amounts of organic matter. Possible black carbonaceous fragments without recognizable forms.

3. Section on northern Hay Island at 0292230, 5100309. *Gyrolithes*, *Teichichnus* and other trace fossils (Fig. 8). Sample SC17-9, with no dispersed organic material. Possible black carbon fragments without recognizable forms.